HELSINKI UNIVERSITY OF TECHNLOGY

Department of Civil and Environmental Engineering

VINCENT FLOQUET

MODELLING CREEP OF SOFT FINNISH CLAY

Final Project submitted on 17/08/2006

SUPERVISOR: Professor OLLI RAVASKA

INSTRUCTOR: Lic.Sc.(Tech) MATTI LOJANDER

ABSTRACT

HELSINKI UNIVERSITY OF TECHNOLOGY
DEPARTMENT OF CIVIL AND ENVIRONMENTAL ENGINEERING
LABORATORY OF SOIL MECHANICS AND FOUNDATION ENGINEERING

ABSTRACT OF THE FINAL PROJECT

Author:	Vincent Floquet		
Project:	Modelling creep of soft Finnish clay		
Date:	17/08/2006	**Number of page:**	70
Chair:	Soil Mechanics and Foundation Engineering	**Code:**	Rak-50
Supervisor:	Professor Olli Ravaska		
Instructor:	Lic.Sc. (Tech) Matti Lojander		

This project was done in the Laboratory of Soil Mechanics and foundation engineering at the Helsinki University of Technology (HUT).

The aim of this project was to study the simulation of settlement in the long term i.e. to understand the creep behavior of clay. Indeed the secondary consolidation is a major concern when buildings, roads, embankments and other structures are founded on deep clay layers. This settlement causes high costs of maintenance in the life span of a structure.

To proceed tests have been carried out in the laboratory and data of former long duration oedometer tests have been gathered. These data have then been processed and analysed in order to extract the right parameters defining the different clays. Once these parameters obtained simulations with PLAXIS' "Soft Soil Creep model" and also classical modelling have been performed. The simulated and observed results have then been compared enabling us to start the reflection about the acquisition of the parameters to model the long term behavior. Attempt to improve this data process, to stick more accurately to the actual behavior, have also been carried out.

PREFACE

I would like to thank Professor Olli Ravaska and Lic.Sc (Tech.) Matti Lojander for their guidance and help that they have given me during this final project. I would also like to thank M.Sc. (Tech.) Timo Stapelfeldt and M.Sc. (Tech.) Hassan Md.Mamunul, from the Helsinki University of Technology, for their time and advice that have been very valuable for me during this project.

In addition, I would like to thank the personnel of the Laboratory of Soil Mechanics and Foundation Engineering at The Helsinki University of Technology and everybody else who have supported me in my work and above all have welcome me so warmly at the laboratory.

Espoo, 17 August 2006

Vincent FLOQUET

LIST OF SYMBOLS

Roman letters

B	$m/r_s = C_\alpha / C_c$
C	$1/r_s$
C	degree Celsius
C_α	secondary compression index
C_c	compression index
C_ε	compression index (%)
C_p	preconsolidation index
C_r	recompression index
C_s	recompression index
c_v	coefficient of consolidation
e	void ratio
e_0	initial void ratio
G	rigidity modulus
H	drainage length
H_0	height of the sample at t=0
H_{EOP}	height of the sample at the end of primary consolidation
K_0	coefficient of earth pressure in consolidated state
K_0	bulk compressibility modulus
k	permeability or coefficient of permeability
k_v	vertical permeability
k_h	horizontal permeability
M	compression modulus, oedometer modulus
m	modulus number
p'_c	preconsolidation pressure
R	time resistance

r_s time resistance number

r_0 initial time resistance number

S settlement

S_f final settlement

Sp preconsolidation pressure

S_p primary settlement

q load

T_v time factor

t time

t_{90} time at 90% of the primary consolidation (=t_v)

t' effective creep time

t_c time to the end of primary consolidation

t_{EOP} time to the end of primary consolidation

t_r reference time

t_0 time when the R-t curve approaches a straight line

u pore water pressure

u' excess pore pressure

u_{cr} pore water pressure due to creep effects

V specific volume

w a force per unit volume

w_L liquid limit

w_N natural water content

Greek letters

α_s coefficient of secondary compression

α_{smax} maximum value of the coefficient of secondary compression

β_{as} coefficient of change in secondary compression

ε strain

ε_e elastic strain

ε_{ep} elastic plastic strain

ε_v vertical strain

ε_c^e elastic strain during primary consolidation

ε_v^{vp} strain corresponding to σ'_p

ε_z^e vertical elastic strain

ε_z^{ep} vertical elastic plastic strain

ε_z^p vertical plastic strain

ε_z^{tp} vertical time-dependant strain

ε_{cr} creep strain

ε_{ac}^{cr} creep strain after primary consolidation

ε_c^{cr} creep strain during primary consolidation

$\dot{\varepsilon}_{ref}$ reference strain rate

$\dot{\varepsilon}_c^e$ elastic strain rate during primary consolidation

$\dot{\varepsilon}_v$ vertical strain rate [1/s]

$\dot{\varepsilon}^{cr}$ creep strain rate

$\dot{\varepsilon}_v^e$ vertical elastic strain rate

$\dot{\varepsilon}_v^{vp}$ viscoplastic strain rate

Γ value of $\log \sigma'_p$ at $\dot{\varepsilon}_v^{vp}$ =10^0 1/s

γ_w unit weight of water

κ elastic stiffness of soil

κ^* modified swelling index

λ elastic plastic stiffness of soil

λ^* modified compression index

μ^* modified creep index

ν_0 coefficient of bulk viscosity

ν_d coefficient of deviatoric viscosity

σ total stress

σ' effective stress

σ'_c preconsolidation pressure

σ'_L effective stress where the compression modulus

σ'_p preconsolidation pressure

σ'_v vertical effective stress (σ_z)

$\dot{\sigma}'_v$ rate of effective stress change

ψ creep parameter, $1/r_s$

τ_c the intercept with the time axis of the straight creep line

Abbreviations

CRS Constant rate of Strain

CPT cone penetration test

EOP end of primary consolidation

EVP elastic viscoplastic

IL increment loading

LIR load increment ratio

OCR overconsolidation ratio

POP preoverburden pressure

TABLE OF CONTENTS

1 INTRODUCTION

The compressibility behaviour of soft soil has been a major concern over the past 100 year. As a matter of fact when buildings, roads, embankments and other structures are founded on deep clay layers we often note that after a long period of time a large settlements occurs. This settlement called creep, causes high costs of maintenance in the life span of a structure. Therefore, it is of great importance to be able to calculate and forecast this settlement occurring in the long term.

The objective of this final project is to strive to understand this phenomenon in order to prevent such damages. The soil studied is the particular Finnish clays coming from different sampling sites of Helsinki neighbourhoods and Finland.

To proceed, the existing theories about the creep behaviour of soft clays have been reminded in the first part of the study, from Karl Terzaghi's first study of consolidation to more modern one, giving thus the basics to understand the phenomenon. Then is exposed a general survey about the tests that had been carried for this work. A focus on the oedometer test (and the long duration procedure) has been made. Indeed it's the most important test that has been carried as most of the data processed come from these tests. Eventually the last part of the study deals with the simulation, either numerical or classical, of Finnish soft clays behavior. The main tool used for this work was the software "PLAXIS". A comparison has been made between the results extracted from the tests (oedometer tests) and the results obtained with the numerical model "Soft-Soil-Creep model" (time dependent behaviour). To carry this analysis, a study of the parameters stepping in the simulation has been made focusing on the way to extract properly these parameters from the tests. An analysis of the results' coherence has led to a notice concerning the validation of numerical computed forecast. Classical simulation has then been carried out to model what couldn't have been regarded with PLAXIS.

2 THEORIES AND MODELS OF THE CONSOLIDATION PROCESS

2.1 The classical consolidation theory

The classical theory of consolidation was developed by Terzaghi (1923) and first published in 1923. Today, this theory is still the foundation of one dimensional consolidation theory. The theory is based on the assumption that there is a unique relationship between effective stress and strain independent of time. Furthermore, Terzaghi assumes that the modulus as well as the permeability is constant with time /Claesson. 2003/.

The assumption that the relationship between stress and strain, or void ratio, is independent of time is a rough simplification used for high plastic clays since those clays show a large amount of time dependent strains. This can be established by laboratory tests, e.g. incremental loading tests.

Terzaghi's equation for one dimensional consolidation can be expressed as:

$$\frac{\partial u}{\partial t} = \frac{M}{\gamma} . \frac{\partial}{\partial z}\left(k . \frac{\partial u}{\partial z} \right) \tag{2.1}$$

or

$$\frac{\partial u}{\partial t} = c_v \frac{\partial^2 u}{\partial z^2} \tag{2.2}$$

if k does not vary with depth,

Where the coefficient of consolidation is defined as:

$$c_v = \frac{k.M}{\gamma_w} \tag{2.3}$$

Where k = permeability [m/s]

M = compression modulus [kPa]

γ_w = unit weight of water [kN/m^3]

The hydraulic conductivity, k, is in the geotechnical field referred to as permeability or coefficient of permeability.

Equation (2.2) is valid under the following conditions:

- The soil is saturated and homogeneous.
- The flow of pore water flow and the strain are one-dimensional.
- Darcy's law is valid
- The change in pore water pressure is equal to change in effective stress.
- The pore water and soil particles are incompressible
- The strain is only dependent on the effective stress

In 1925 Terzaghi introduced the first oedometer device and suggested a test procedure where a specimen is loaded step-wise, each load step doubling the previous value, until the excess pore pressure has dissipated. For clays, duration of 24H is quite common. This procedure is still widely used, and is commonly referred to as an incremental load oedometer test.

In 1936 Terzaghi proposed a model for calculating the degree of consolidation
Figure (2.1)
The degree of consolidation is determined by calculating the time factor T_v:

$$T_v = \frac{c_v}{H^2}.t \qquad (2.4)$$

Where c_v = coefficient of consolidation [m^2/s]

H = drainage length [m]

T = time [s]

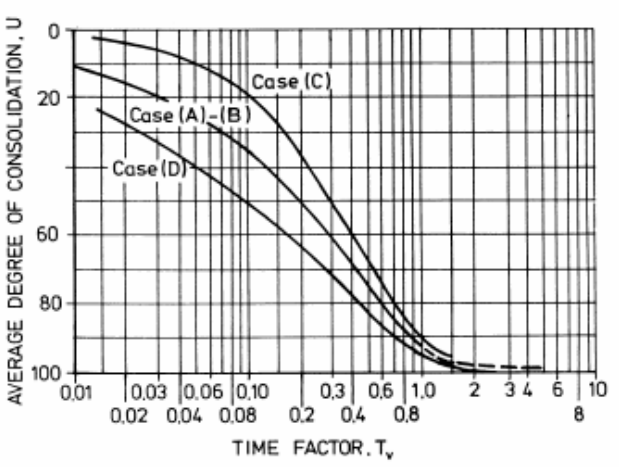

Figure 2.1 Relationship between time factor and degree of consolidation. The three curves correspond to three different cases of excess pore pressure and drainage conditions.

Casagrande (1936) proposed an oedometer test procedure for determining the end of primary consolidation, EOP, of each load increment, i.e. when the excess pore pressure has completely dissipated.

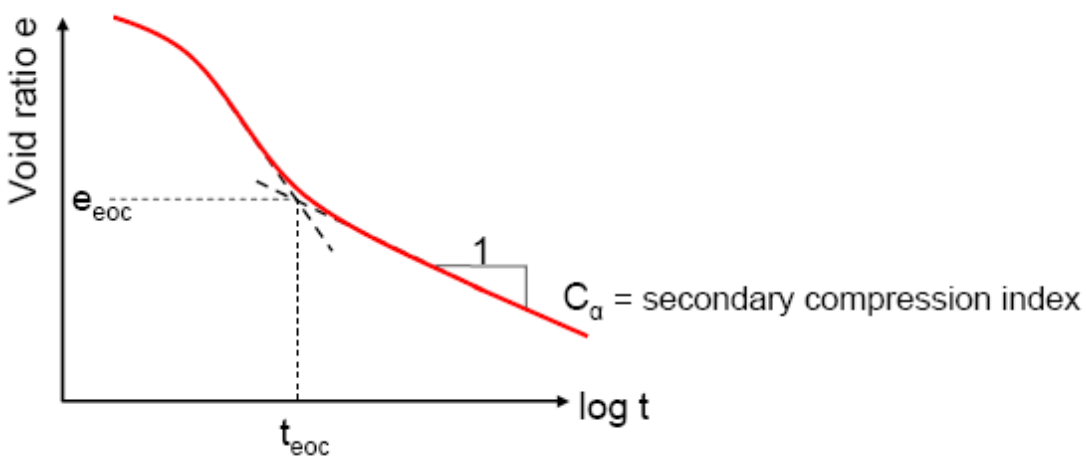

Figure 2.2 Casagrande method of determining EOP, 100% of primary consolidation.

It assumes that time-strain curve is plotted in a semilogaritmic diagram: The EOP is defined as the point of intersection between the two tangents of the curve as shown in Figure 2.2.

Another commonly used method of determining the EOP was suggested by Taylor (1948). In this method the strain is plotted versus the square root of time.

2.2 Early models for consolidation including creep effects

Originally, consolidation settlements were calculated according to Terzaghi's theory and possibly creep settlements starting after the full excess pore pressure dissipation has occurred, e.g. Buisman (1936). Taylor and Merchant (1940) formulated the first theory where creep effects were at least partly involved in the process of dissipation of excess pore pressure. Two years later, in 1942, Taylor developed a first model of a generation variation of void ratio, e, versus effective stress, σ', and time, t. The model was applicable for oedometer tests.

When the consolidation models have been presented in the literature, the consolidation process has almost always been divided into primary and secondary consolidation. The basics assumption is that the primary consolidation occurs during an increase of the effective stress and a simultaneous decrease of the excess pore pressure and volume. The process of secondary consolidation is defined as a decrease in volume under constant effective stress. Over a long period of time creep strains were separated from the primary consolidation. In 1957, Suklje presented a model, described below, where creep strains also was assumed to occur during primary consolidation. This is the dominating concept for models presented over the 20-30 years.

The model presented by Suklje (1957), where the relationship between effective stress, void ratio and strain rate defined the consolidation curve. This relationship was presented by the set of isotaches.

Suklje was the first to suggest that the behavior of clay at a one-dimensional compression is governed by a unique relationship between effective stress, void ratio and strain rate. The model developed by Suklje assumes that creep occurs during the entire consolidation process. It thus assumes that primary consolidation and creep effects are not two separate processes, occurring before and after the dissipation of excess pore pressure. Suklje also accounted for the fact that that the time dependent

strains are influenced by the thickness of the clay layer, permeability and drainage conditions.

2.3 The Bjerrum model

In 1967 Bjerrum presented a conceptual model, which, in a similar fashion to Suklje's model, also assumes that primary consolidation and creep strains are not divided into separate processes /Bjerrum 1974/. It should be observed that the model is primarily intended for settlements that have developed for a long period of time, i.e. a period of time in a geological perspective. The engineer however, is normally concerned with a shorter period of time, often 50-100 years or shorter. Consequently, in engineering practice, it is essential that the design takes account of the time delay caused by permeability and the drainage conditions.

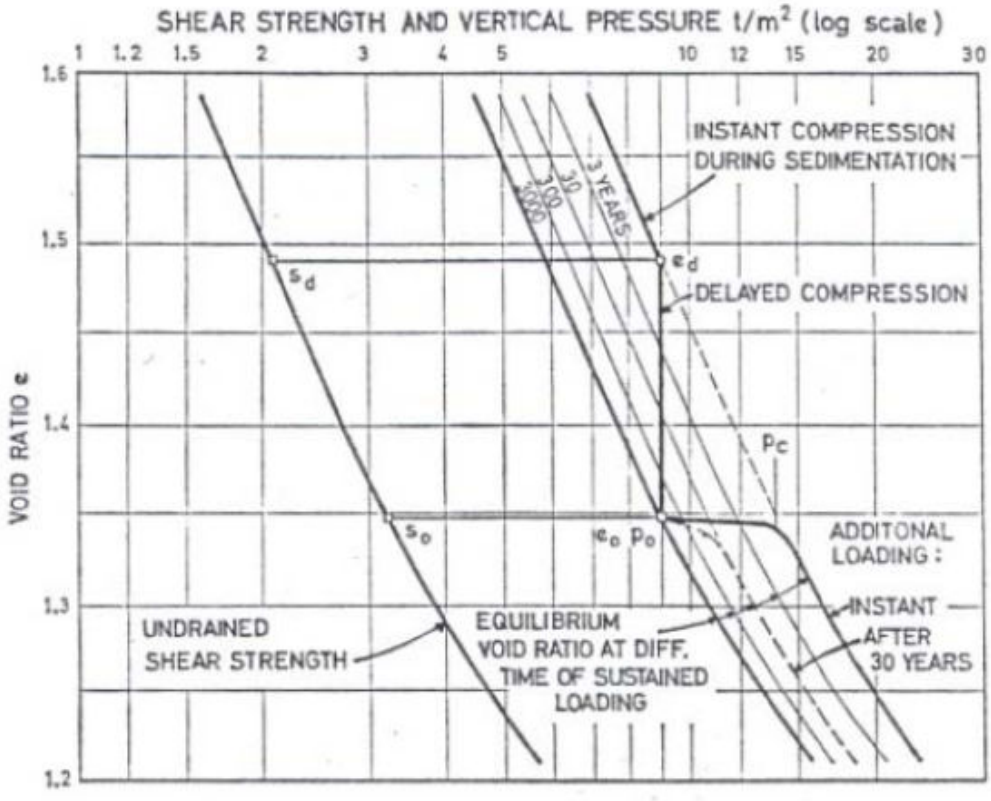

Figure 2.3 Diagram describing the conceptual model developed by Bjerrum. Series of parallel time lines describing the compressibility and shear strength of clay, which shows delayed consolidation.

The Bjerrum model was intended to explain the apparent preconsolidation pressure or overconsolidation ratio of virgin clays, resulting from geological ageing. The model also explains settlements and creep effects occurring over time, in spite of the fact that the preconsolidation pressure has not been exceeded. In figure 2.3 the unique relationship between void ratio, pressure (effective stress) and time is represented by a series of parallel time lines on the vertical pressure-void ratio diagram. Bjerrum separated strains into “instants” and “delayed” compression and used “time lines” to model the reduced creep rates resulting from the increased duration of loading.

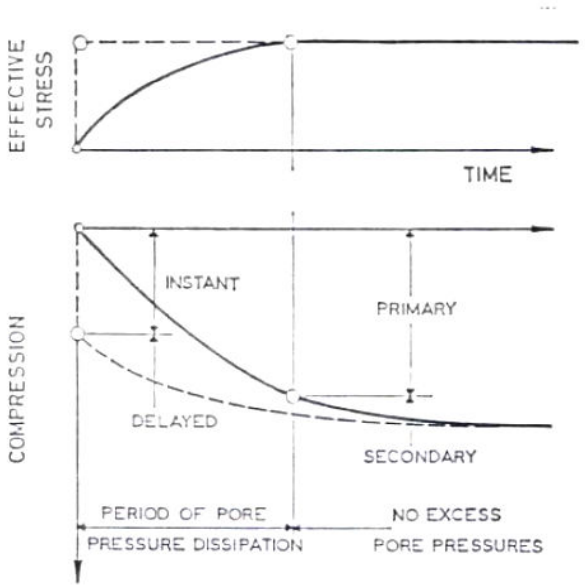

Figure 2.4 Definition of the two parts of settlements, “instant” and “delayed” compression, compared with “primary” and “secondary” compression illustrated by the broken and the solid line respectively (Bjerrum, 1967).

Figure 2.4 shows how the compression of a clay layer is assumed to develop in time for an applied load if the applied load is transferred instantaneously to the clay structure, i.e. as effective stress This is termed instant compression and the broken lines curve illustrates how the strains would occur if the pore water in the saturated clay could be disregarded. The subsequent compression, i.e. under unchanged effective stress, is the delayed compression. Due to the viscosity of water the effective stresses will gradually increase when the excess pore pressure dissipates and consequently compression will occur along the solid line.

Bjerrum (1967) also stated that there is an obvious relation between preconsolidation pressure and undrained shear strength. The relation is assumed to remain unchanged at changing void ratio (or strain). Hence, a decrease in void ratio, or increasing strains, increases the undrained shear strength. The magnitude of the overconsolidation ratio, OCR, depends, according to Bjerrum, on the plasticity of the clays and its geological history.

2.4 The creep parameter C_α and α_s

A widely used parameter for describing the creep behavior of clay is the *secondary compression index*, C_α, defined as(according to Taylor):

$$C_\alpha = \frac{\Delta e}{\Delta \log(t)} \tag{2.5}$$

where e = void ratio

The creep parameter that is commonly used in Sweden, the *coefficient of secondary consolidation*, α_s relates to the *secondary compression index*. The only difference in the definition of the two parameters is that is described C_α as a function of strain,ε and α_s as a function of void ratio, e /Larsson.1986/. The relationship between the two creep parameters can be expressed as:

$$\alpha_s = \frac{C_\alpha}{1 + e_0} \tag{2.6}$$

where $1 + e_0$ = the specific volume, V

e_0 = initial void ratio

The coefficient of secondary compression, α_s, is thus defined as:

$$\alpha_s = \frac{\Delta \varepsilon_{cr}}{\Delta \log(t)} \tag{2.7}$$

Where α_s = coefficient of secondary compression

ε_{cr} = creep strain

t = time

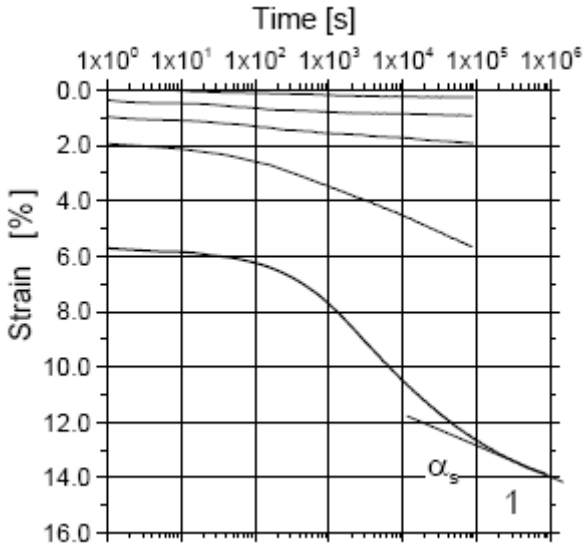

Figure 2.5 Evaluation of α_s from an incremental loading test

The creep behavior is often described by the coefficient of secondary compression, α_s, as a function of strain. Figure 2.6 shows a general model of α_s and its variation with strain. The coefficient β_{as} define the change in α_s with increasing strain /Larsson.1986/.

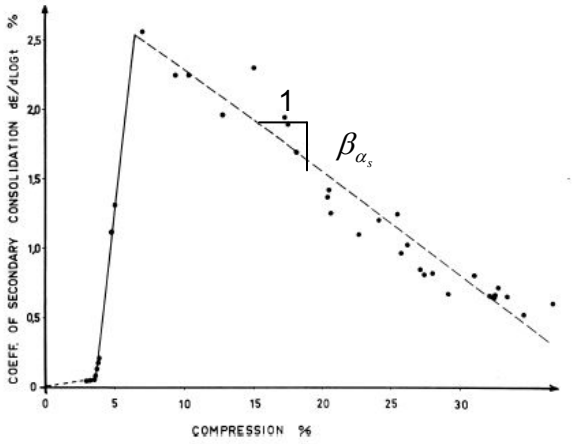

Figure 2.6 The model of the coefficient of secondary compression, α_s.

2.5 The time resistant concept

Another parameter that described the creep behavior is the time resistance, R, introduced by Janbu (1969). If an applied stress is to be considered as an action, then the stress will be considered as a reaction. In the case of creep, the time will be considered as an action and the creep strain is its reaction. This relationship is defined as:

$$R = \frac{dt}{d\varepsilon} \tag{2.8}$$

where R = time resistance [s]

ε = strain

In laboratory tests it has been found that the time resistance of clays increases about linearly with time, as is illustrated in Figure 2.7, and can be expressed as:

$$\frac{dR}{dt} = r_s \tag{2.9}$$

where r_s is the time resistance number.

It can be seen from Figure 2.7 that after a certain time t_0 the time resistance is assumed to increase linearly with time /Svanø & Christensen 1991/. Thereafter the relation may be expressed:

$$R = r_s.(t - t_r) \tag{2.10}$$

where t = time

t_r = reference time

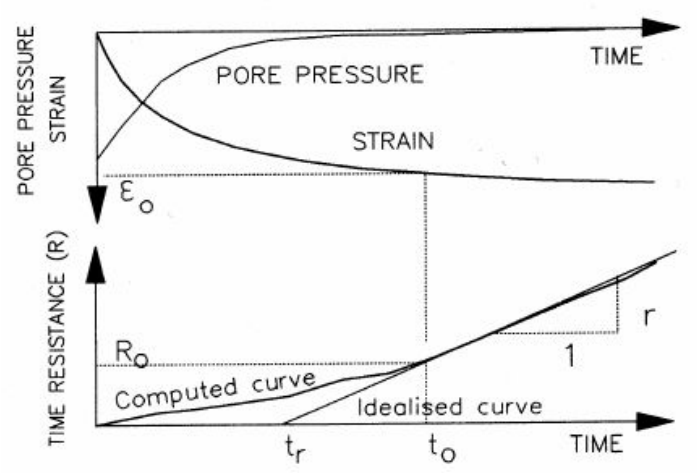

Figure 2.7 *Time resistance as a function of time for one load increment (Svano et al, 1991).*

The creep strain rate $\dot{\varepsilon}$ at time is equal to the inverse of the time resistance R:

$$\dot{\varepsilon}_{cr} = \frac{\partial \varepsilon_{cr}}{\partial t} = \frac{1}{R} = \frac{1}{(t - t_r)} \tag{2.11}$$

where $\dot{\varepsilon}_{cr}$ = creep strain rate [1/s]

ε_{cr} = creep strain

By integration of equation (2.11) from t_0 to t, the strain due to creep can be expressed as:

$$\Delta\varepsilon_{cr} = \frac{1}{r_s}\int_{t_0}^{t}\frac{dt}{(t - t_r)} = \frac{1}{r_s}\ln\frac{t - t_r}{t_0 - t_r} \tag{2.12}$$

where t_0 = time when R-t curve approaches a straight line

From equation (2.12), the time resistance number, r_s, can hence be defined as:

$$\frac{1}{r_s} = \frac{\partial \varepsilon_{cr}}{\partial \ln t} \tag{2.13}$$

Finally the relationship between the time resistance and the coefficient of secondary consolidation is given by:

$$\alpha_s = \frac{\partial \varepsilon_{cr}}{\partial \log(t)} = \frac{\partial \varepsilon_{cr}}{\partial \ln(t)} . \frac{\partial \ln(t)}{\partial \log(t)} = \frac{\partial \varepsilon_{cr}}{\partial \ln(t)} . \ln 10 \tag{2.14}$$

$$\alpha_s = \frac{\ln 10}{r_s} \approx \frac{2.3}{r_s} \tag{2.15}$$

2.6 Relationship between parameters for primary and secondary consolidation

A parameter commonly used worldwide to describe the compression behavior of clay for effective stresses greater than the preconsolidation pressure is the compression index, C_c, which is defined as:

$$C_c = \frac{\Delta e}{\Delta \log \sigma'} \tag{2.16}$$

where e = void ratio

Mesri and Godlewski (1977) claimed that there is a unique relationship between C_α and C_c that holds true for any type of soil and that will be valid for any kind of combinations of time, effective stress and void ratio:

$$\frac{C_\alpha}{C_c} = constant \tag{2.17}$$

For a majority of inorganic soft clays the relationship equals (Mesri and Castro, 1987):

$$\frac{C_\alpha}{C_c} = 0.04 \pm 0.01 \tag{2.18}$$

In 1985 Janbu defined the relation between the *modulus number*, *m*, and *time resistance number*, r_s, as:

$$\frac{C_\alpha}{C_c} = \frac{m}{r_s} \tag{2.19}$$

where $m = \dfrac{M(\sigma')}{\sigma'}$

M(σ') = oedometer modulus [kPa]

σ' = effective stress [kPa]

The stiffness of the clay is assumed to increase linearly with stress in the normally consolidated domain, i.e., M = m.σ'. This is in accordance with the concept of Janbu's tangent modulus.

As has been shown, the three creep parameters described in this section are strongly related to each other, despite the fact that there can be some significant differences.

Appendix 1: The relationship between effective stress, strain and strain rate
The effect of temperature on the compressibility
Determination of the creep parameter from CRS tests

3 OEDOMETER TESTS-EXPERIMENTAL RESULTS

3.1 Operating method

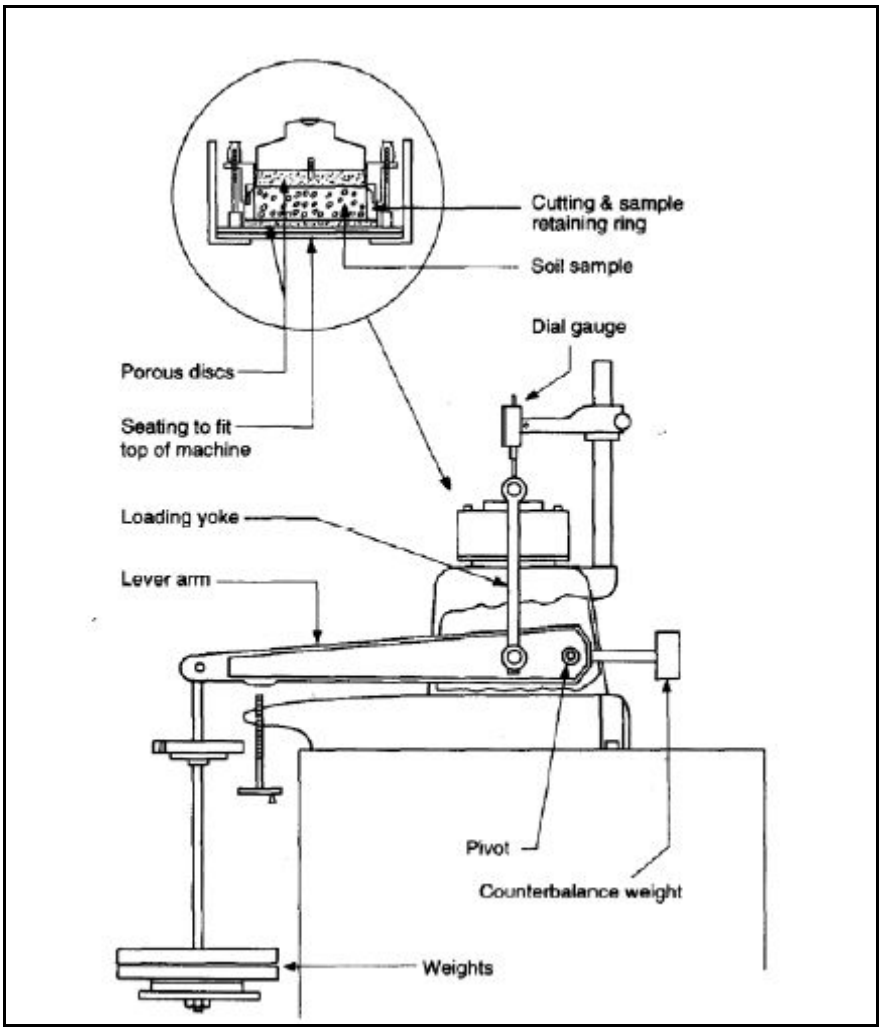

Figure 3.1 Oedometer apparatus

The Casagrande oedometer test is most widely used. The apparatus (see figure 3.1) consists of a cell which can be placed in a loading frame and loaded vertically. In the cell the soil sample is laterally restrained by a steel ring, which incorporates a cutting shoe used during specimen preparation. The top and bottom of the specimen are placed in contact with porous discs, so that drainage of the specimen takes place in the vertical direction when vertical stress is applied; consolidation is then one-dimensional.

To run this test a standard procedure is to follow. In this procedure the specimen is subjected to a series of pre-selected vertical stresses each of which is held constant while dial gauge measurements of vertical deformation of the top of the specimen are made, and until movements cease (normally 24 h and several weeks for long-time test). Dial gauge readings are taken at standard intervals of time after the start of the test (i.e. 0, 6, 15 and 30s, 1, 2, 4, 8, 15, 30 and 60mm, 2, 4, 8 and 24h). At the same time that the first load is applied, the oedometer cell is flooded with water, and if the specimen swells the load is immediately increased through the standard increments until swelling ceases.

There is different kind of oedometer tests (Increment load IL, constant rate of strain…). The one I have carried out is the standard incremental loading test. The principle is to proceed with applying at each step a double load increment than the current one. For each phase values (height of the sample or strain) are checked and plotted. The stabilisation of the settlements indicates us that a new load increment is to be put. To study the behavior of clay in the long run, tests were carried out (for the last load increment) from 30 to 100 days."

Figure 3.2 Oedometer test in the laboratory

3.2 Results processing – Curves fitting

For this project, I have carried out a long duration oedometer test, Otaniemi 4702, and I have processed also the results of former oedometer tests. Here are the tests considered, some characteristics and their references:

Table 3.1 Main characteristics of the tests

Reference number	Sampling site	From (load)	To (load)	σ_1 [kPa]	Original depth	Sample type	Duration-load step σ_1 [days]
806	Otaniemi	6,25	200	25	2,32 – 2,35	2	70
116	Perno	12,5	800	25	1,75 – 1,77	1	55
21D1	Taasia	100	1600	100	4,42 – 4,45	2	90
26B1	Taasia	50	1600	100	3,47 – 3,50	2	100
4452	Vanttila	3,57	84	42	2,64 – 2,67	3	68
4453	Vanttila	3,57	84	42	1,64 – 1,66	3	67
4072	Otaniemi	5,35	342,4	42,8	1,90 – 1,92	3	7

Sample type 1: h_0 = 1,88 cm; A = 45,7cm^2

Sample type 2: h_0 = 2 cm; A = 20 cm^2

Sample type 3: h_0 = 1,5 cm; A = 13,82 cm^2

(See Appendix 2, Sampling)

3.2.1 Determination of the coefficient of consolidation c_v, the coefficient of secondary compression C_α, the end of primary consolidation time t_{EOP} and the height at the end of primary consolidation H_{EOP}

The results of each loading stage of an oedometer test are normally plotted in a chart representing the dial gauge readings either as a function of square root of elapsed time, or as a function of the logarithm of elapsed time. The coefficient of consolidation (c_v) used in calculations of settlement can be obtained from these curves, using Taylor and Merchant's method, or Casagrande's method respectively. C_α and the characteristic EOP parameters are also obtained thanks to these curves.

Example:

For the test 4452 on the sample from Vanttila site here is how the data are determined (end of primary consolidation EOP, consolidation coefficient c_v, C_α):

For each load step we plot the height-time (log(t):Casagrande; sqrt(t):Taylor) curve.

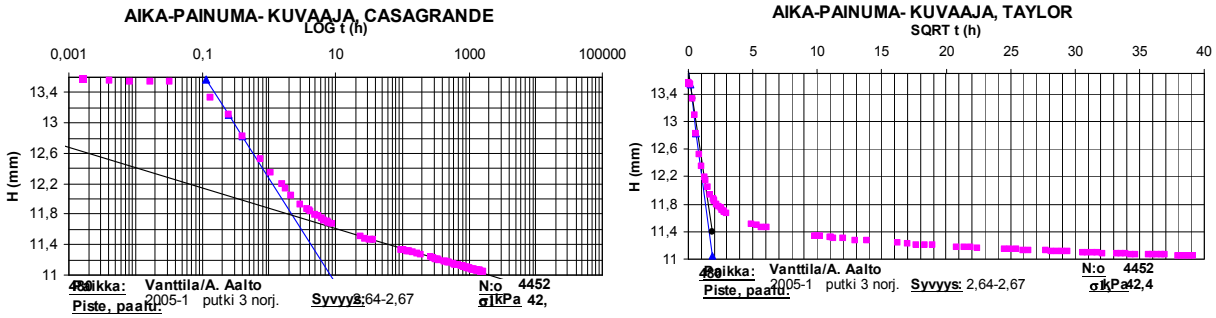

Figure 3.3 Determination of the characteristic EOP parameters, Cv and Cα - Fifth Load step: 42,4 kPa of Vanttila 4452

For the load step σ_1 we assess the value of C_α and c_v (with the Casagrande's and the Taylor's method):

3.2.1.1 Casagrande's method

The logarithmic method consists in plotting the deformation-time dependency in a semi-logarithmic scale. The consolidation coefficient itself is determined from the relation:

$$c_v = \frac{T_{50}.H^2}{t_{50}} \qquad (3.1)$$

where T_{50} is a time factor corresponding to 50% primary consolidation and where t_{50} is the time necessary for reaching 50% consolidation.

The time factor T_{50} = 0.197. For a sample drained at both sides, the height H equals half of the sample's height.

$$c_v = \frac{0{,}197.H^2}{t_{50}} \qquad (3.2)$$

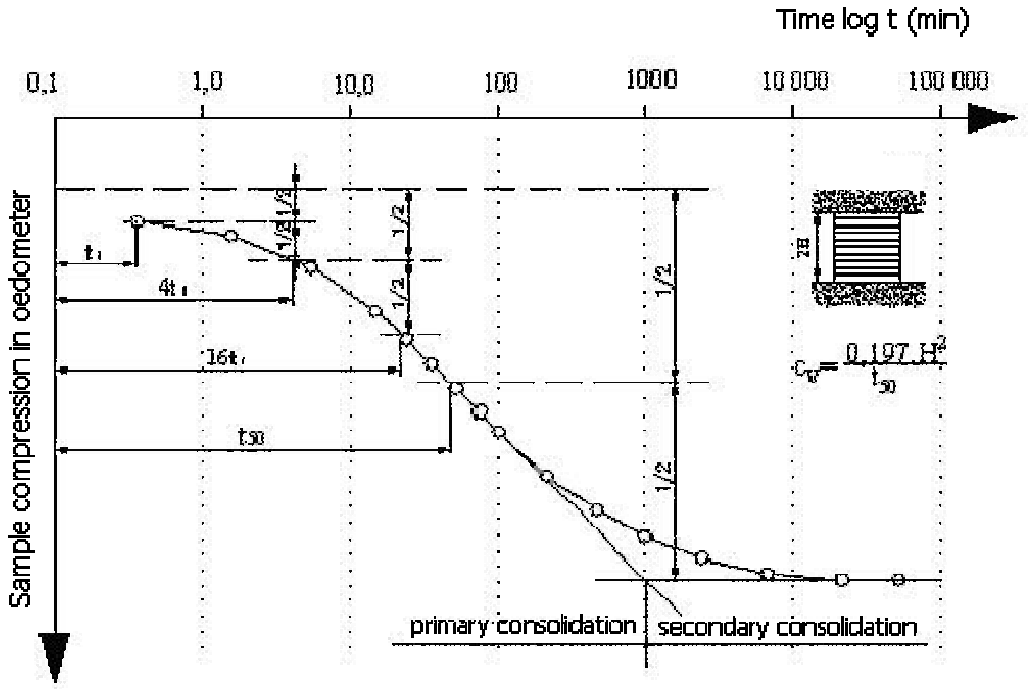

Figure 3.4 Time-deformation logarithm dependency

In order to be able to determine t_{50}, we must first find the beginning of primary consolidation and the inflexion point of the medium part of the consolidation curve and a line running along the straight section of the last part of the curve. This point is considered to be the end of primary and the beginning of secondary consolidation. As can be seen from the figure 3.4, the time at 50% consolidation is given by the intersection point of a parallel line to the axis x and the consolidation line, the parallel line with the axis x being exactly in the middle of deformation, between the beginning and the end of primary consolidation. The beginning of primary consolidation may be found e.g. by plotting the time 16t and its quarter 4t, and it further holds true that the distance between these two times on the vertical axis equals ½ of total deformation reached in the time 16t from the beginning of primary consolidation.

Here with the Casagrande's method: c_v = 0,13 m^2/a

N.B:

The last part of the some curves plotted in Figure 3.5 shows an increased slope. This can be explained by local stress relaxation and hence an increase in the heights of energy links of the slip units. This is akin to work-hardening, e.g. as in metals. Indeed a critical number of slip units is reached and domains formation stops leading to an accelerating creep rate followed by complete failure. But this phenomenon can also be explained by the formation of high local stress point which makes the energy barriers among slip units decreased, this outweighs the creep effects due to domains formation /Pusch 1978/. Modelling this behavior has been studied in chapter 5.

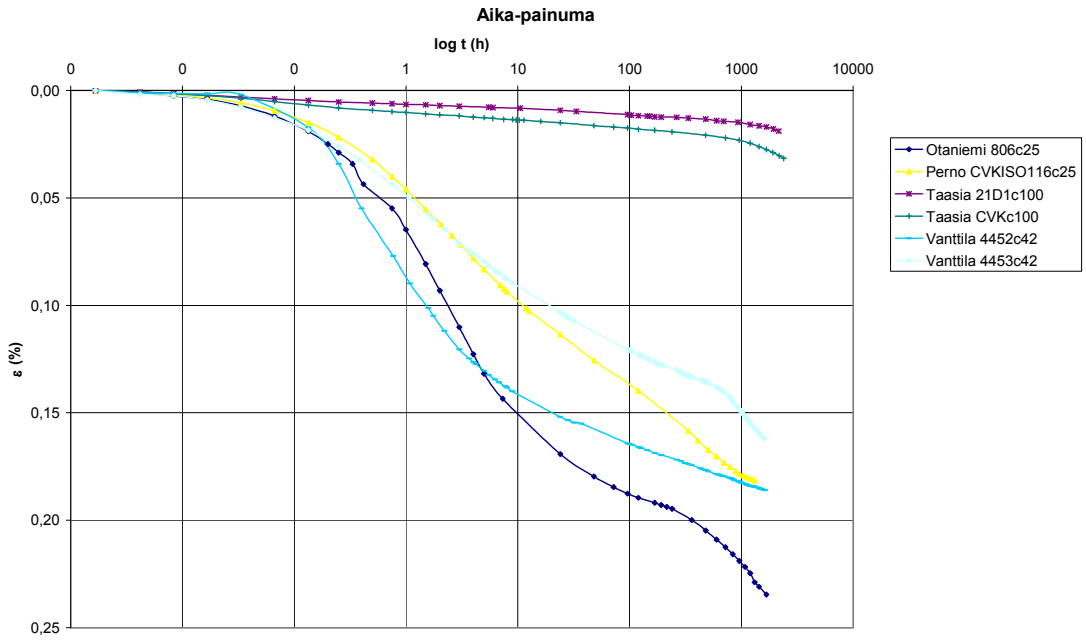

Figure 3.5 Strain-log(t) curves of the different studied tests

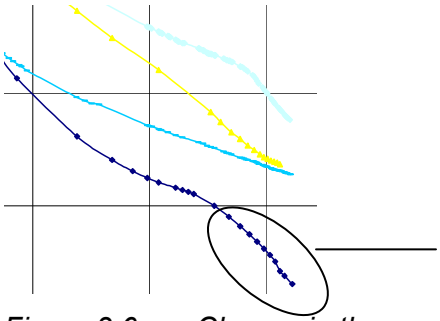

Local stress points formation ►► heterogeneity

Figure 3.6 Change in the creep slope

3.2.1.2 Taylor's method

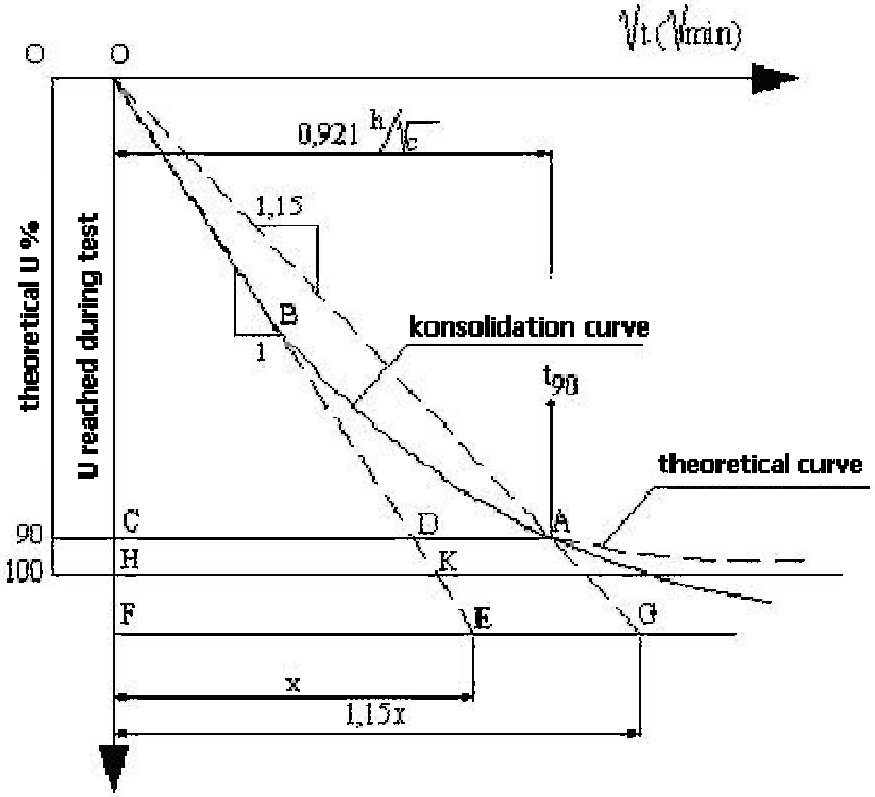

Figure 3.7 Determination of c_v

Taylor's method is very commonly used. Time is plotted on the horizontal axis in the form of a root of t, while deformation is plotted on the vertical axis. The intersection point of the tangent to the linear section of the consolidation curve with the vertical axis is considered to be the beginning of primary consolidation. A line with a tangent 1.15 times greater than the above-mentioned tangent is led through the point ds. The method presumes that this line intersects the consolidation curve at a point which corresponds to 90% consolidation. Numerical solution of uniaxial consolidation may be performed analytically by using Fourier series (Taylor, 1948). It is presumed that the experimental curve for the point A is identical to the theoretical curve (A representing 90% consolidation).

Thus, if we know the time factor we may determine the consolidation coefficient from the relation 3.3:

$$c_v = \frac{0{,}848.H^2}{t_{90}} \qquad (3.3)$$

where H is the half of the sample's height in [m]; t_{90} is the time at reaching 90% consolidation in [s] and T_{90}=0,848 is the time factor at this same time.

A condition of great importance in using Taylor's method is that the test sample should be fully saturated

Here with Taylor's method: c_v = 0,22 m^2/a

3.2.2 Determination of the preconsolidation pressure σ'_p, the compression index C_c and the swelling index C_s

The results of all the oedometer load stages are normally combined in one graph of void ratio as a function of the logarithm of effective pressure (figure below), constructed on the basis of the calculated void ratios at the end of each of the load stages (or with the EOP value). These results are also used to calculate the coefficient of compressibility (m_v = Δe/(1 + e_o).(1/Δp), where Δe is the void ratio change for a pressure change Δp) which is used to predict the magnitude of settlement. This is carried out for each load stage. Coefficient of compressibility results are seriously affected by sample disturbance in soft or sensitive clays, and by sample size effects in hard clays and soft rocks.

We can now model the behavior of clay with load with two methods more or less useful and accurate. The first model rely on Janbu's equation and aims at modelling the bend of the curves plotted on the $e-\sigma_1$ chart. To proceed we use TAMO (in-plant program) from which we get the parameter m_1, β_1, m_2, β_2 characteristic parameters for Janbu's model of the consolidation. The second model, more classical, uses two straight lines, the coefficient of which are C_c and C_s (or C_r). This modelling is less accurate and so on not reliable concerning determination of the preconsolidation pressure.

Janbu's model

σ_{v0} `(kPa)=	0	β_1 =	-0,595	β_2 =	1,185
σ_P (kPa)=	13	m_1 =	9,39	m_2 =	49,8

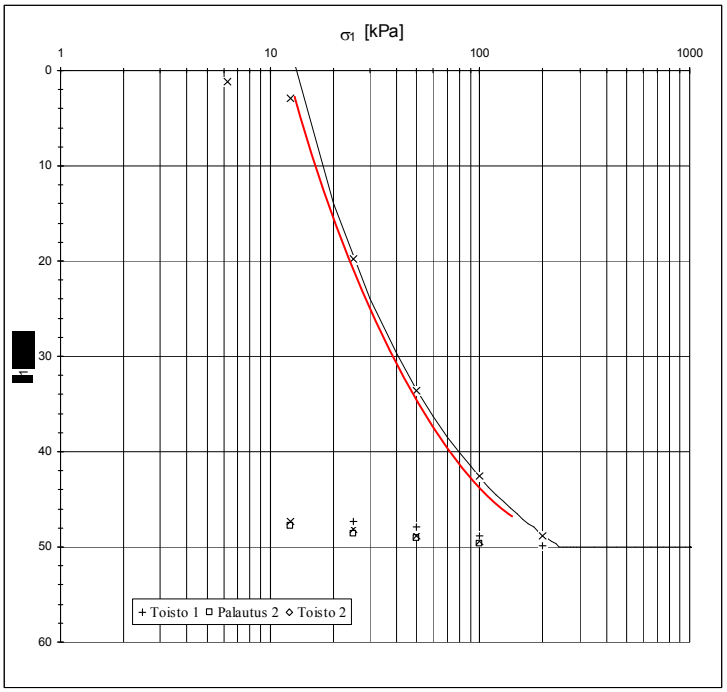

parameter m,β,C :

$$\varepsilon_1 = \frac{1}{m\beta}\left(\frac{\sigma}{\sigma_v}\right)^{\beta} + C_1, \text{ if } \beta \neq 0$$

$$\varepsilon_1 = \frac{1}{m}\ln\left(\frac{\sigma}{\sigma_v}\right) + C_1, \text{ if } \beta = 0$$

Classical model

σ_{v0} `(kPa)=	0
σ_P (kPa)=	13

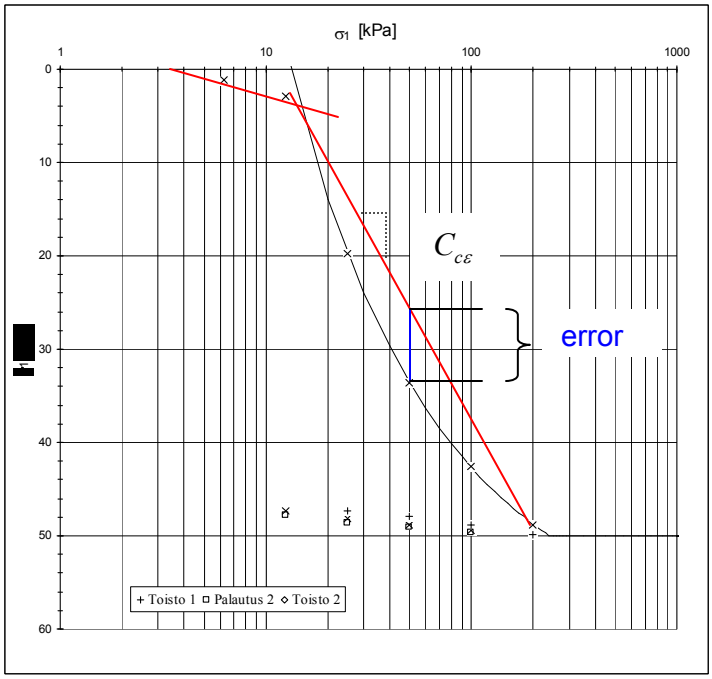

parameter C_c, C_s

$$C_s(or.C_c) = \frac{\Delta e}{\Delta \log \sigma_1}$$

$$C_{c\varepsilon} = \frac{\Delta \varepsilon_1}{\Delta \log \sigma_1}$$

Figure 3.8 Models comparison of clay's behavior

The trend curves stick more to the real phenomenon when modelled by Janbu's equation taking into account the bend of the curve. That's why we prefer using this model and proceeding as proposed by A.Aalto & M.Lojander & O.Ravaska to determine the preconsolidation pressure /A.Aalto &M.Lojander & O.Ravaska 2004/. However the classical modelling is necessary because the parameters got from this model are of use in many consolidation model and FEM software (e.g. PLAXIS).

We can now determine the preconsolidation pressure thanks to these charts obtained with Janbu's modelling.

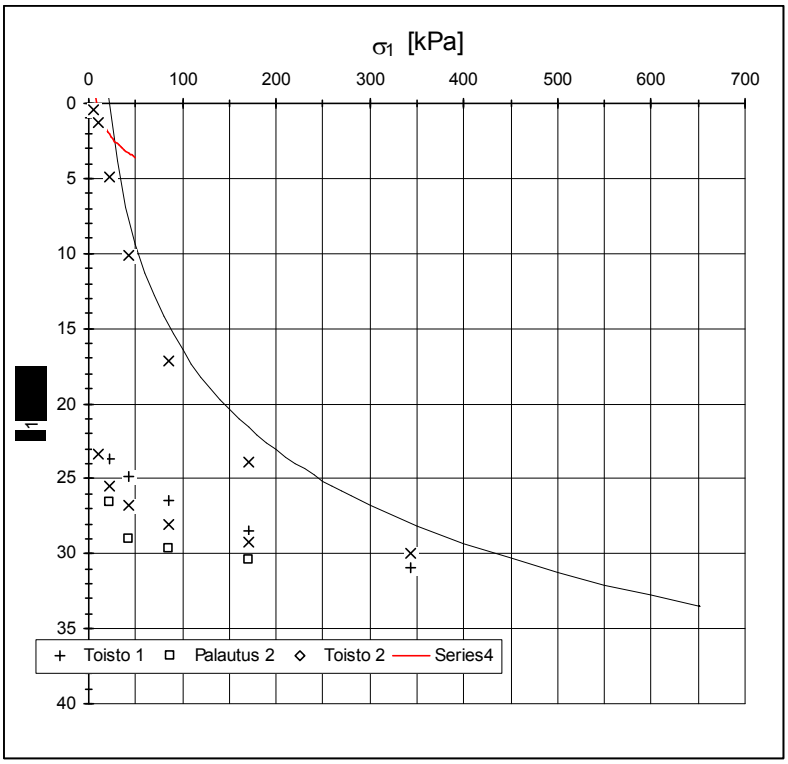

Figure 3.9 Preconsolidation pressure determination on Otaniemi 4702

The preconsolidation pressure is here 31 kPa. Note that the value is widely influenced anyway by the point chosen to model the trendline.
At the end of the test the sample is weighed then dried and weigh again thus we can assess the water content of the sample and its void ratio.

N.B: In order to proceed the numerical modelling of the oedometer test we need to get the values of the Cam-Clay swelling index κ, the Cam Clay compression index λ, and the modified creep index μ. This has been done manually by converting the parameters as explained in chapter 4.

Appendix 2: Sampling
Classification data
Other tests

4 NUMERICAL MODELLING: PLAXIS SIMULATION OF OEDOMETER TESTS

4.1 The Plaxis Soft Soil Creep Model (Buisman model)

4.1.1 Model's equation

The principle of the calculation is based on Buisman creep model. Of course this model has been improved all along the year to come to this one. It has been improved thanks to the work of researchers like Bjerrum, Garlanger or Mesri. Eventually the model was implemented in Plaxis in 1998 thanks to the work of Vermeer et al. and Neher & Vermeer /PLAXIS-material models manual/.

The basic equation of the model is the following one:

$$\varepsilon^H = \varepsilon_c^H - C.\ln\left(\frac{\tau_c + t'}{\tau_c}\right) \tag{4.1}$$

Where ε^H is the logarithmic strain defined as

$$\varepsilon^H = \ln\left(\frac{V}{V_0}\right) = \ln\left(\frac{1+e}{1+e_0}\right) \tag{4.2}$$

And

$C = \dfrac{C_\alpha}{(1+e_0).\ln 10}$ is a modification of the compression index

t' is the effective creep time: t' = t - t_c (see fig 4.12)

and τ_c the time up to the strain rate starts decreasing (we can however assess $\tau_c = t_c$)

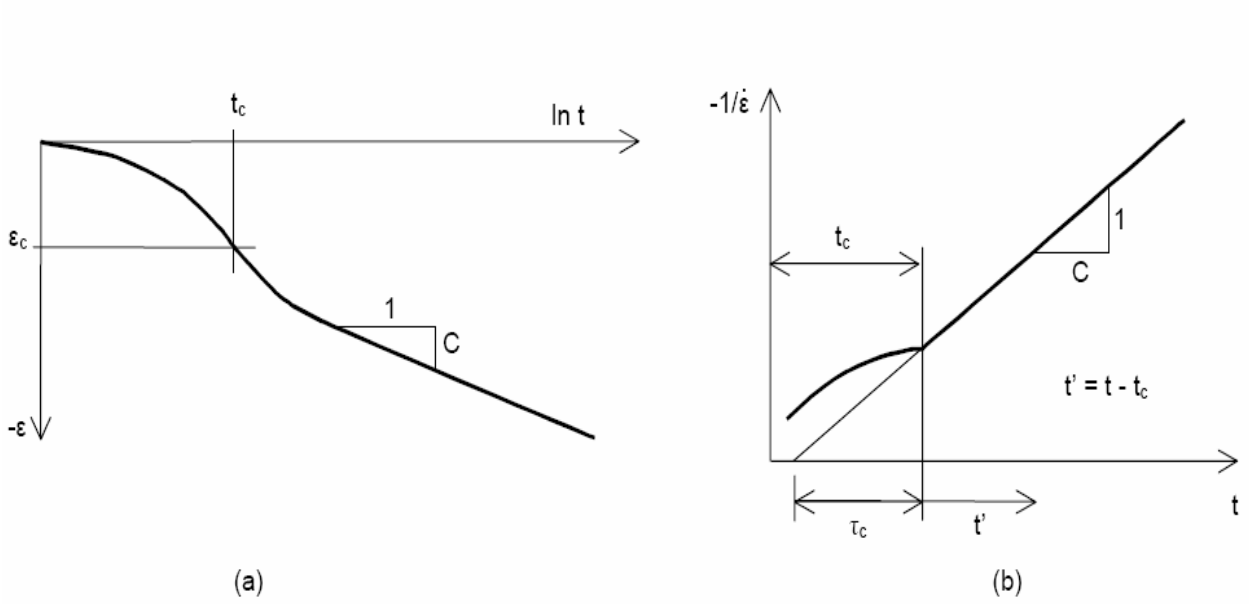

Figure 4.1 Consolidation and creep behaviour in standard oedometer test

From this model are adapted the two main equation used to compute the results:

$$\varepsilon = \varepsilon^e + \varepsilon^c = -A.\ln\left(\frac{\sigma'}{\sigma_{0'}}\right) - B.\ln\left(\frac{\sigma_{pc}}{\sigma_{p0}}\right) - C.\ln\left(\frac{\tau_c + t'}{\tau_c}\right) \tag{4.3}$$

And the differential law following:

$$\dot{\varepsilon} = \dot{\varepsilon}^e + \dot{\varepsilon}^c = -A\frac{\sigma'}{\sigma'} - \frac{C}{\tau}\left(\frac{\sigma'}{\sigma_p}\right)^{\frac{B}{C}} \tag{4.5}$$

In which A, B, C are customised constants described as following:

$$A = \frac{C_r}{(1+e_0).\ln 10} \tag{4.6}$$

$$B = \frac{C_c - C_r}{(1+e_0).\ln 10} \tag{4.7}$$

$$C = \frac{C_\alpha}{(1+e_0).\ln 10} \tag{4.8}$$

And

σ' the final effective loading pressure

$\sigma_{0'}$ the initial effective pressure before loading

σ_{pc} the preconsolidation pressure at the end of consolidation

σ_{p0} the preconsolidation pressure before loading

4.1.2 Particular model's parameters

The parameters used in Soft-Soil-Creep model are not the one we usually find in the literature. Most of the time, using Janbu's model (cf. 3.3.2) is more accurate to simulate the behavior of the clay. However we are using here parameters resulting from the classical model (with a straight line):

- Modified compression index, λ^*

$$\lambda^* = \frac{\lambda}{1+e_0} \tag{4.9}$$

See Figure 4.2 below.

- Modified swelling index, κ^*

$$\kappa^* = \frac{\kappa}{1+e_0} \tag{4.10}$$

Usually the value of kappa is determined by the same method. However the different values used to plot the trendline are extracted thanks to an unloading-reloading process. When such a process is not carried out we can assess the value of κ in the range [λ /10 ; λ /5].

κ and λ value are both extracted from the lnσ1-volumetric strain plot (v=1+e).

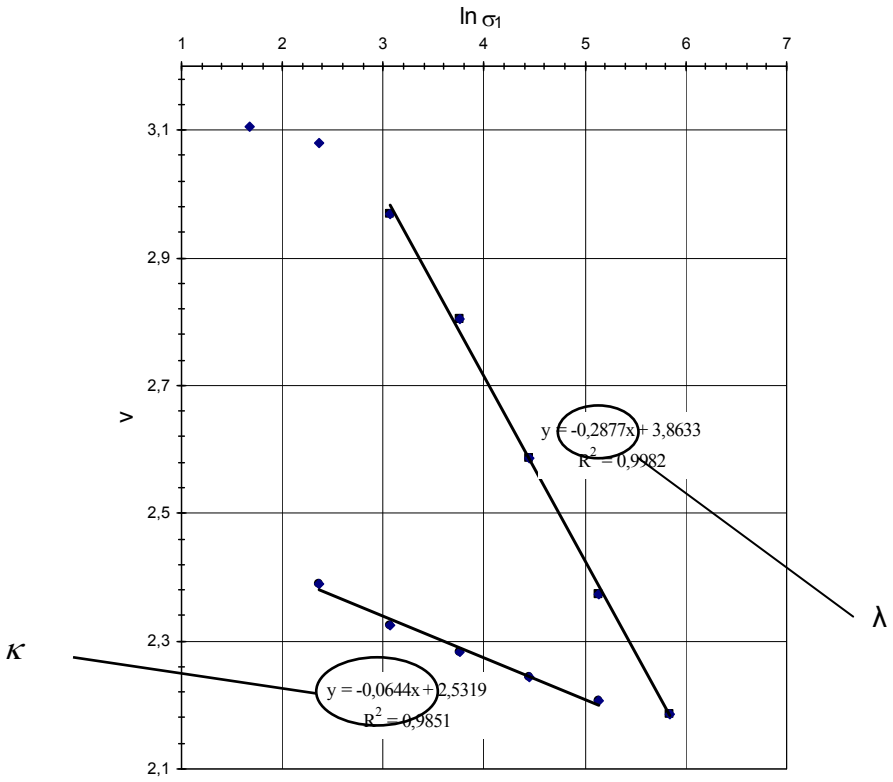

Figure 4.2 Determination of lambda and kappa parameters

They are then converted into κ^* and λ^* as explained before-mentioned.

- Modified creep index, μ^*

$$\mu^* = \frac{C_\alpha}{(1+e_0).\ln 10} \tag{4.11}$$

The secondary compression index, C_α, is extracted from the oedometer test data processed as explained below. See Figure 4.3.

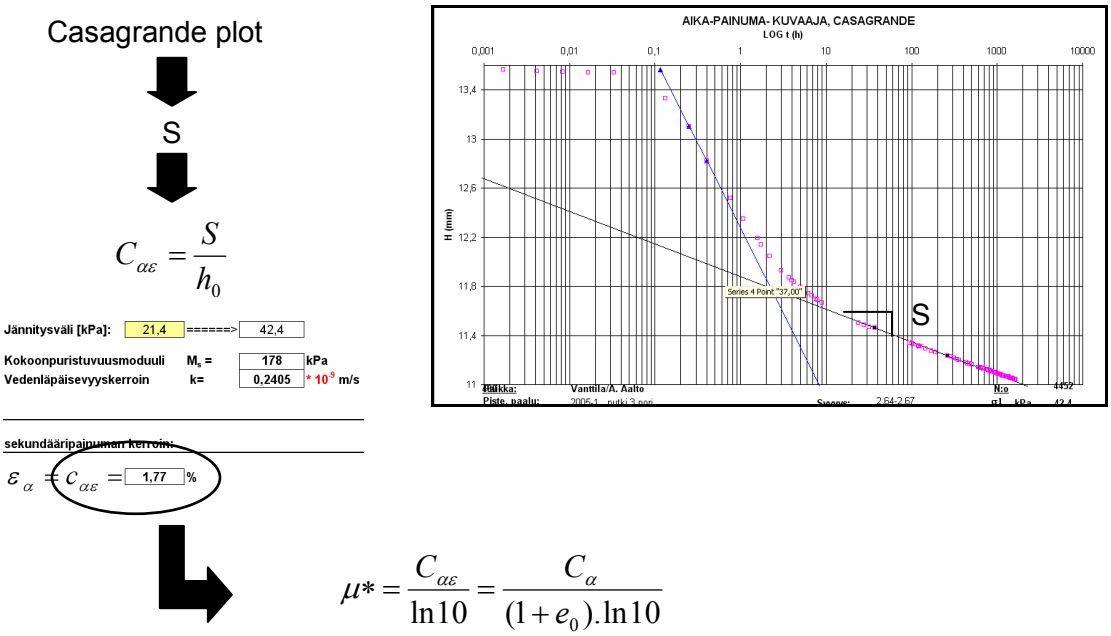

Figure 4.3 Determination of the μ parameter*

We can note that the parameters c and φ (stabilization parameters) are of no use in this analysis.

4.1.3 Parameters' influences

- Modified compression index, λ^*

λ^* is an equivalent parameter to C_c. It means that the higher the parameter is the steeper is the second part of the curve in the Casagrande construction.

- Modified swelling index, κ^*

κ^* is an equivalent parameter to C_s. The modified swelling index is of great importance when it deals with excavating or clearing away. But it is also of importance when modelling oedometer tests. Indeed the swelling compression index is one of the main parameter that enables us to assess the instant compression. The higher κ^* is the bigger instant compression is. This phenomenon is more noticeable when modelling drained materials.

- Modified creep index, μ^*

μ^* is an equivalent parameter to C_α. Thus the higher this coefficient is the steeper the final part of the slope is.

- Permeability, k

The permeability influences widely the delay of the compression. Indeed a high value of k means that the water can circulate easily in the soil enabling the pore water pressure to dissipate quickly. On the contrary a low value of k will prevent pore water pressure to dissipate that quickly. On the plot we can notice this phenomenon by a shift in time.

4.2 Calculated/Observed data comparison for the different oedometer tests.

4.2.1 Oedometer tests simulation

In order to model properly the oedometer test we use these specific features.

- axisymmetric model.
- horizontal and vertical displacement blocked at the foot of the sample.
- horizontal displacement blocked at the sides of the sample.
- water level set at the upper side of the sample (saturated sample).
- upper and lower side drained.
- material behavior: Undrained.
- side boundaries closed for consolidation and water flow.
- application of the load trough a infinitely rigid plate (very high young modulus)
- instant application of the load then consolidation phase as long as desired.

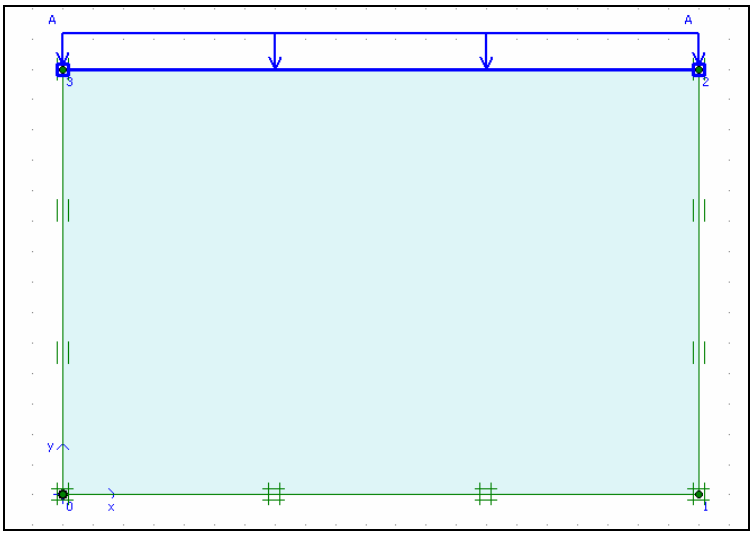

Figure 4.4 Boundary conditions of the model

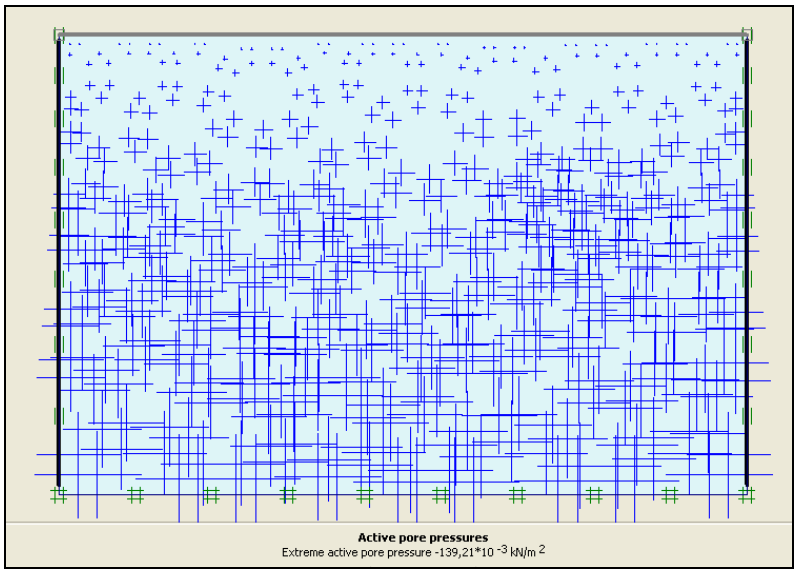

Figure 4.5 Initial water pressure (sample undrained)

N.B:

The mesh generation is not of big importance in this model as the shape is simple. A coarse mesh is thus accurate enough.

4.2.1.1 Otaniemi 4702

4.2.1.1.1 Parameters

- Dimensions of the sample:
  - H_{init} =15 mm

- A = 1382 mm^2

- $\sigma_1 = \sigma$ applied = 42,8 kPa
- $\sigma_{10} = \sigma$ applied at the previous load step = 21,4 kPa
- h_0 = height of the sample at the end of the previous load step = 14,265 mm

- k = 3,65.E-5 m/day.
- e_0 = 2,12
- $POP = \left|\sigma_p - \sigma_{yy}^{'0}\right| = \left|25 - 0\right| = 25kPa$

- c = 2 kPa
- φ = 24˚
- ψ = 0˚

- γ_{sat} = 15,45 kN/m^3
- γ_{unsat} = 8,64 kN/m^3

4.2.1.1.1.1 *Modified compression index, λ**

For this modelling a study on the influence of the method to get the lambda and kappa value has been carried out.

Indeed to get these values we plot the $\sigma_1 = v(voumetric\_strain = 1 + e)$ but the value of the settlement can be taken at different time and give thus different value of the slope (λ). One has plotted the value of the volumetric strain for each load step at : the end of the load step (7 days), 1 days and 2,4 hour. Thus we have obtained different values of lambda depending on the way to process the test's data. / Perrone. 1998/

If we plot the time line for this test according to Bjerrum's concept we obtain Figure 4.6 below:

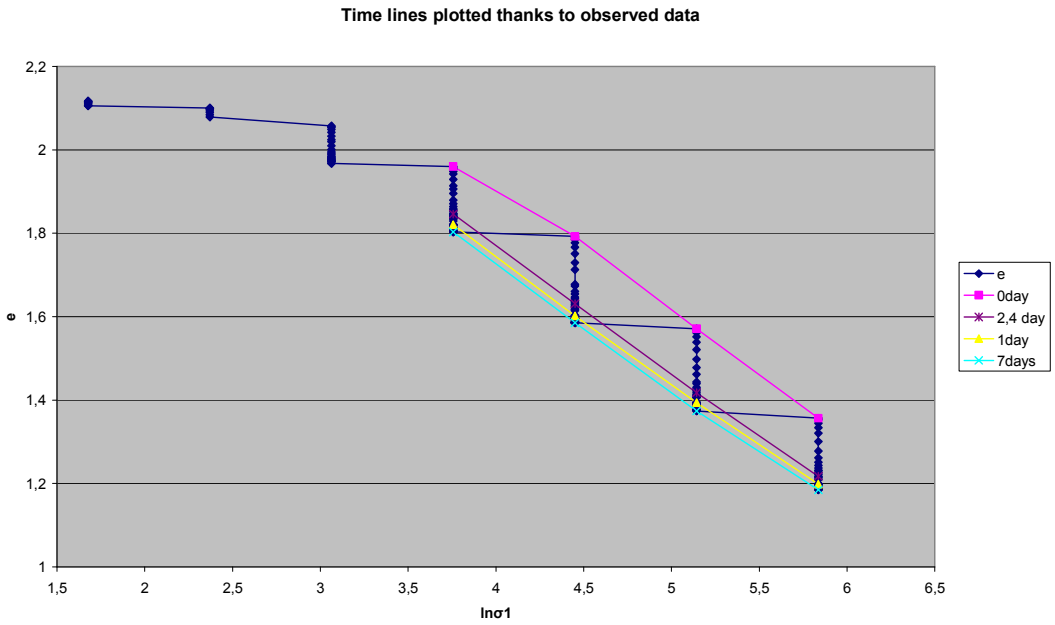

Figure 4.6 Bjerrum time lines observed for 4702 oedometer test

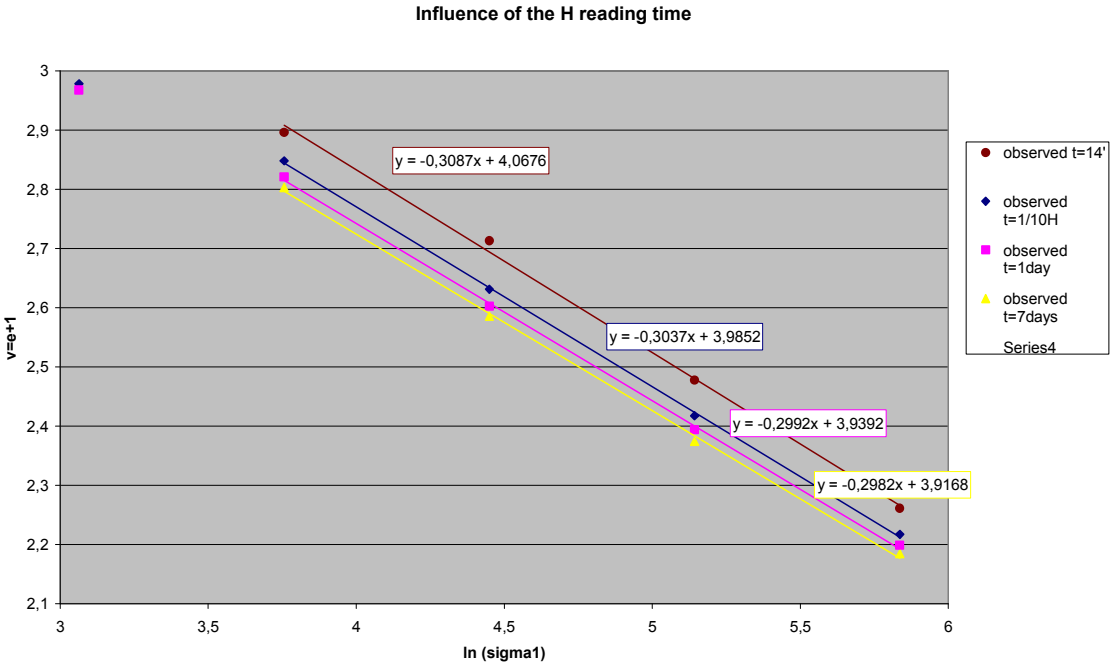

Figure 4.7 Assessment of the lambda coefficient in the course time resulting from Bjerrum's chart

This coefficient (λ) decreases all the more if you assess its value late in time during the settlement of a load stage as we can see on Figure 4.8:

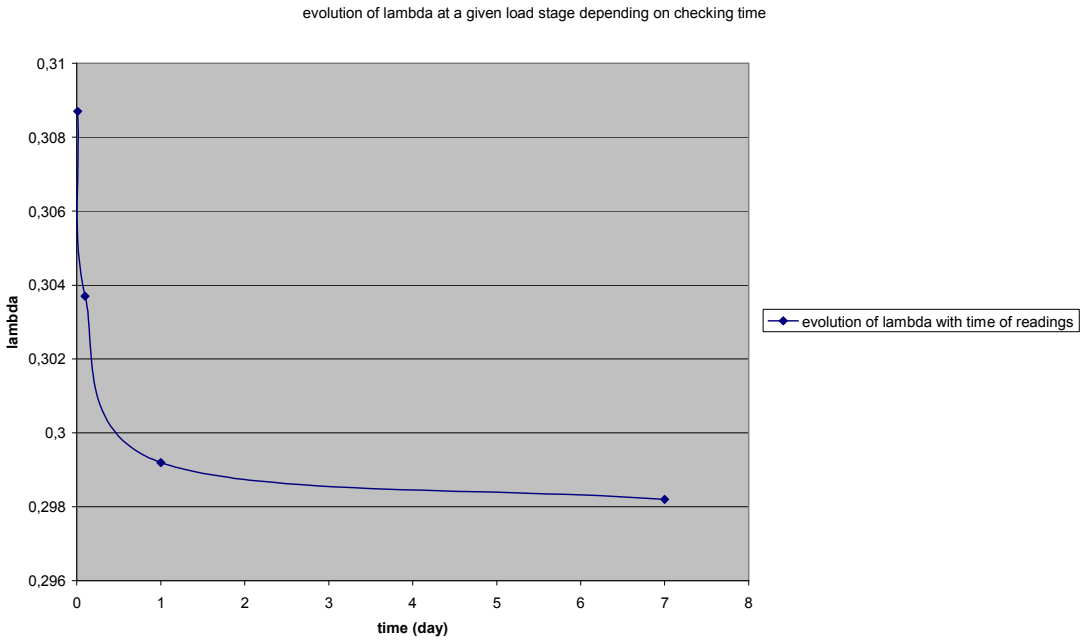

Figure 4.8 Evolution of the lambda value with time

4.2.1.1.1.2 Modified swelling index, κ*

The second aspect of the study regards the way to assess the value of κ. Indeed the unloading curve is not really a straight line so if we only take the very first points to assess the slope, the value of κ will be lower than if we regard every points of the unloading stage (see figure 4.9).

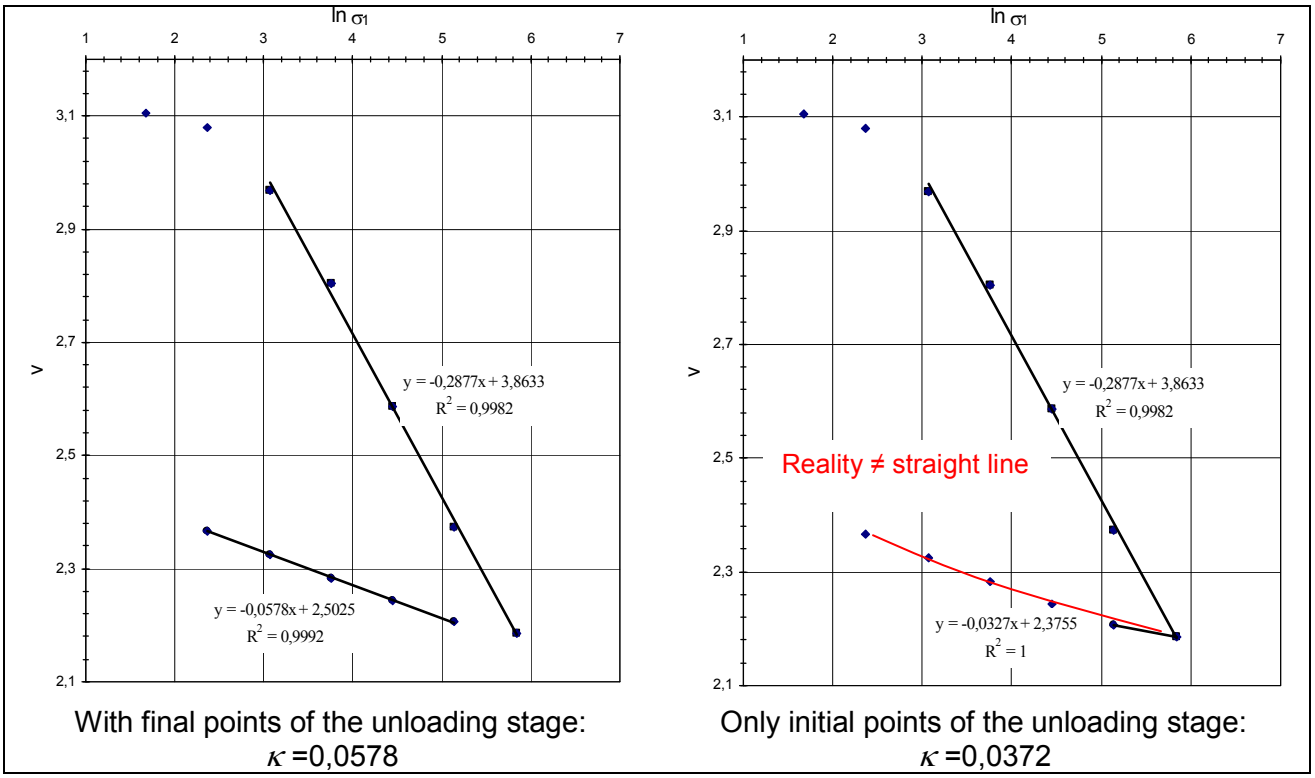

Figure 4.9 Influence of the points considered to model the slope of the recompression line

Eventually the set of parameters $\lambda - \kappa$ can be summed up in this table:

Table 4.1 Set of parameters lambda, kappa

		λ	κ	λ^*	κ^*	λ / κ
Settlement at final time	κ init	0,2877	0,0327	9,22.E-2	1,05.E-2	8,78
	κ all	0,2877	0,0578	9,22.E-2	1,85.E-2	5
Settlement at t=1 day	κ init	0,2833	0,0123	9,08.E-2	3,94.E-3	23
	κ all	0,2833	0,0578	9,08.E-2	1,85.E-2	4,9
Settlement at t≈2,4H	κ init	0,2815	Default 0,0327	9,02.E-2	1,05.E-2	8,6
	κ all	0,2815	0,0578	9,02.E-2	1,85.E-2	4,9

4.2.1.1.1.3 Modified creep index, μ* (C_α)

The goal of this study is to uproot errors coming from subjective plotting of C_α trendline.

According to Mesri and Godlewski, the value of the ratio Cα/Cc should be constant and equal to 0,04±0,01. In this study we will try to estimate the value of C_α after a one day-long test, the value after a 7 day-long test (value obtained by assessing the slope

regarding the height at 6 days and 7 days) and eventually the value of C_α that best fits to the entire curve.

Example: Load step 42,8kPa

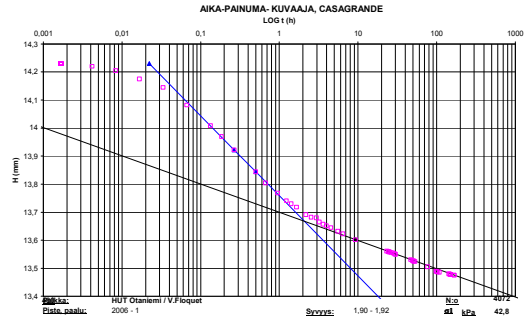

1day assessment: C_α =0,67

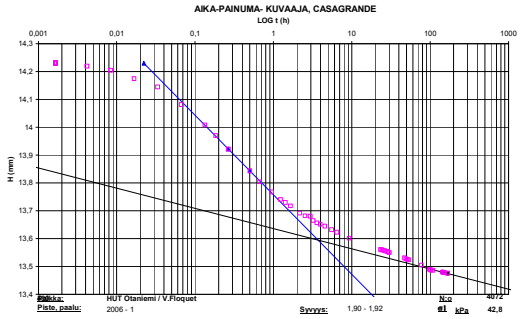

7 days assessment: C_α =0,48

Figure 4.10 C_α assessment.

Table 4.2 Set of parameters C_α

Load step (kPa)	$C_{\alpha e}$ 7day (%)	C_α 7day (%)	$C_{\alpha e}$ 1day (%)	C_α 1day (%)	$C_{\alpha e}$ 7day best fitted slope (%)	C_α 7day best fitted slope (%)
42,8	0,48	0,01498	0,67	0,0209	0,68	0,021216
85,6	0,2	0,00624	0,82	0,02558	0,68	0,021216
171,2	0,52	0,01622	0,73	0,02278	0,76	0,023712
342,4	0,53	0,01654	0,6	0,01872	0,51	0,015912

N.B: “Best fitted slope” is obtained regarding all points of the test and plotting the curves

We should now assess the value of parameter λ at each stage of the test, to be able to determine its variation with the course of time and thus the variation of C_α / C_c ratio.

To assess the value of the λ coefficient at each step we use a linear regression on the two points (before and at the load step considered):

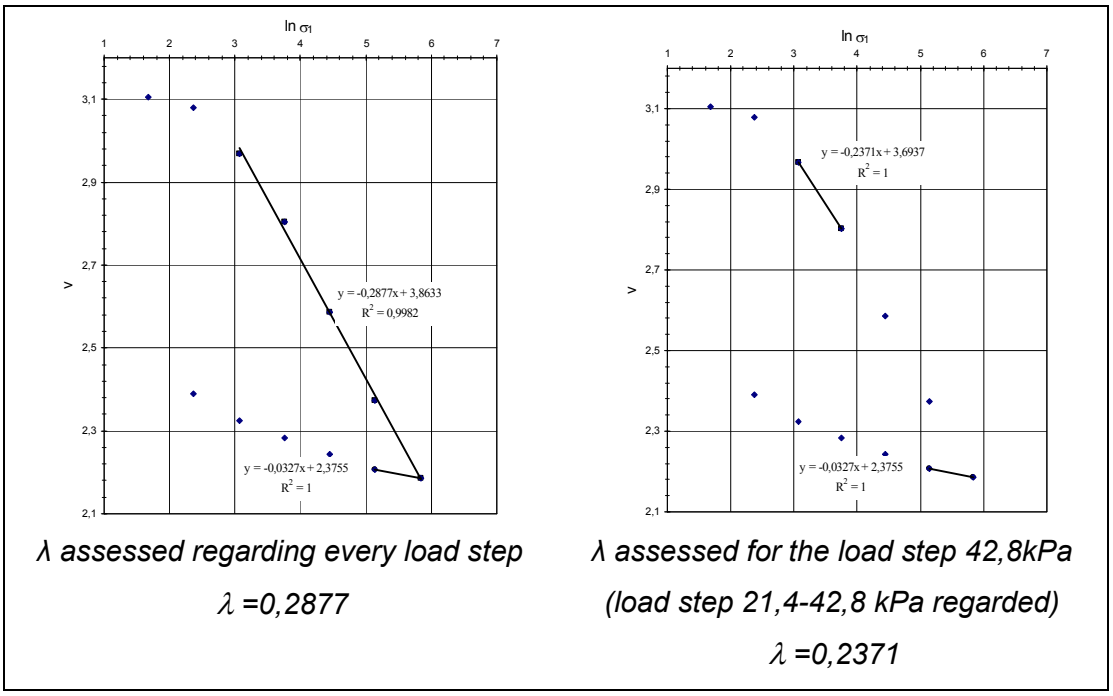

λ assessed regarding every load step

λ =0,2877

λ assessed for the load step 42,8kPa

(load step 21,4-42,8 kPa regarded)

λ =0,2371

Figure 4.11 λ assessment

The values of λ are acquired this way for each load step. Here is the table compiling the values:

Table 4.3 set of λ value at each load step

Load step [kPa]	42,8	85,6	171,2	342,4
λ	0,2371	0,3139	0,3049	0,2734

Here are the results of the study (plotted with C_α value obtained in Table 4.2):

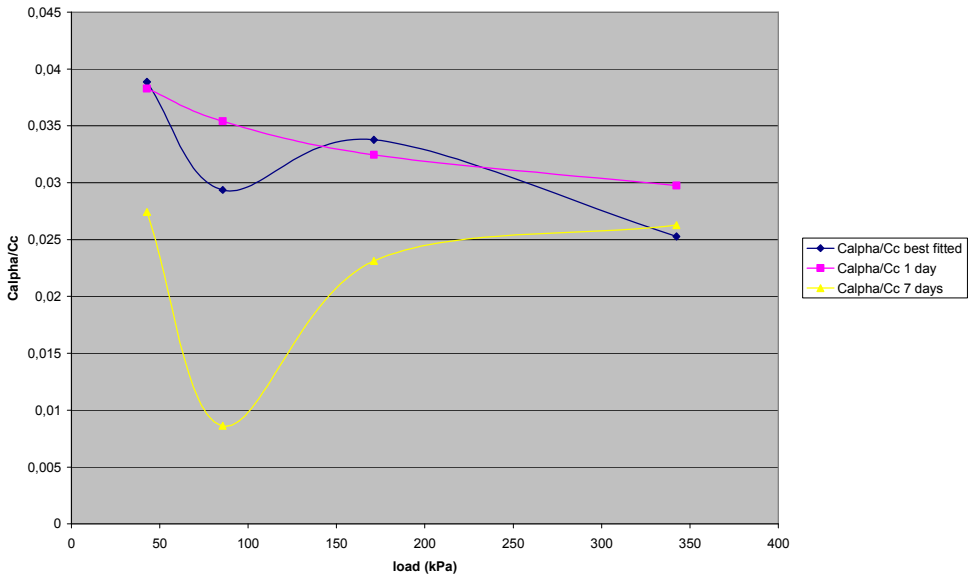

Figure 4.12 C_α / C_c variation with load

One can notice that the value of C_α/C_c is far from being constant all along the test. However for the value "best fitted after 7 days" and "1day test" the ratio stays in the range predicted by Mesri and Castro (0,04±0,01).

Now let's try to get a constant ratio. Let's study the case "best fitted curve" and try to improve our method to plot the slope of the secondary consolidation.

First we calculate the average value of Cα/Cc:

$$C\alpha / Cc_{average} = \frac{0{,}03886 + 0{,}02935 + 0{,}03377 + 0{,}02528}{4} = 0{,}03182$$

If we try to follow Mesri's assumption we can get the value of C_α thanks to the value of lambda checked:

Table 4.4 C_α values corrected according to Mesri's assumption

Load step (kPa)	Cc (local)	Calpha resulting	Calphae resulting (%)	Calphae observed	Errors plotting the slope (%)
42,8	0,545943	0,017372	0,556791791	0,68	-22,1282
85,6	0,722781	0,022999	0,737144426	0,68	7,752134
171,2	0,702058	0,022339	0,716009351	0,76	-6,14387
342,4	0,629527	0,020032	0,642036591	0,51	20,56528

Let's see the difference induced by the correction of the slopes on the Casagrande's construction for some load steps.

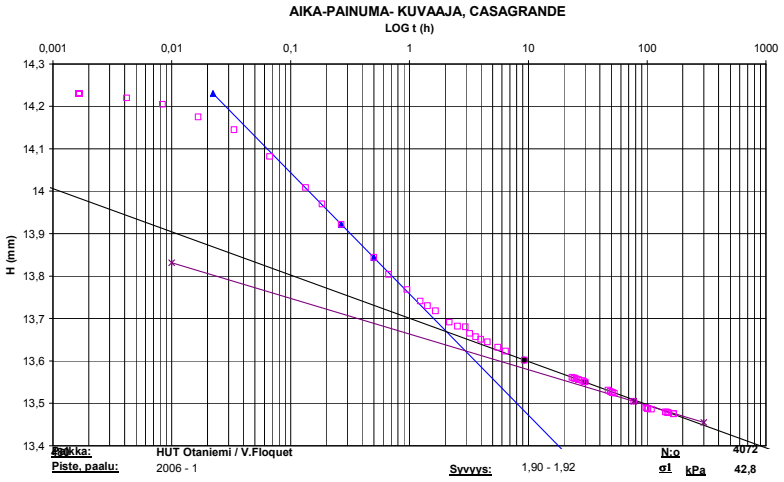

Figure 4.13 C_α slope, best fitted/corrected (Load step 42,8kPa)

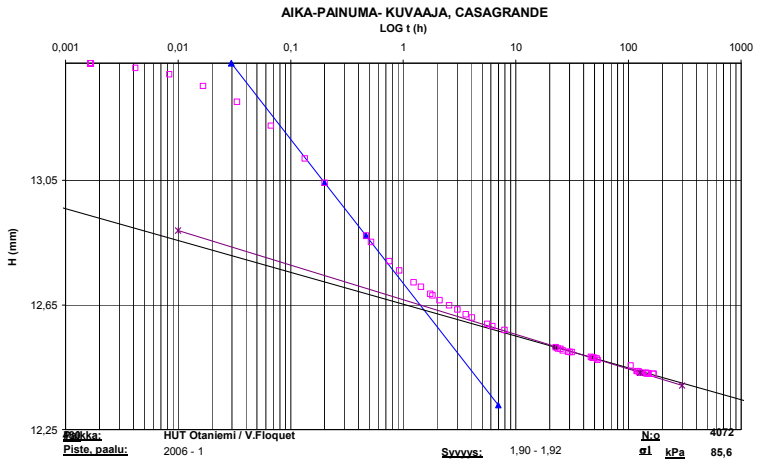

Figure 4.14 C_α *slope, best fitted/corrected (Load step 85,6kPa)*

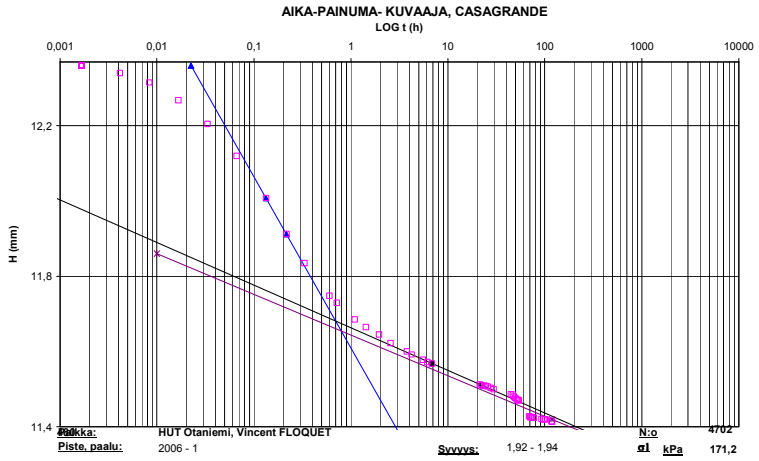

Figure 4.15 C_α *slope, best fitted/corrected (Load step 171,2kPa)*

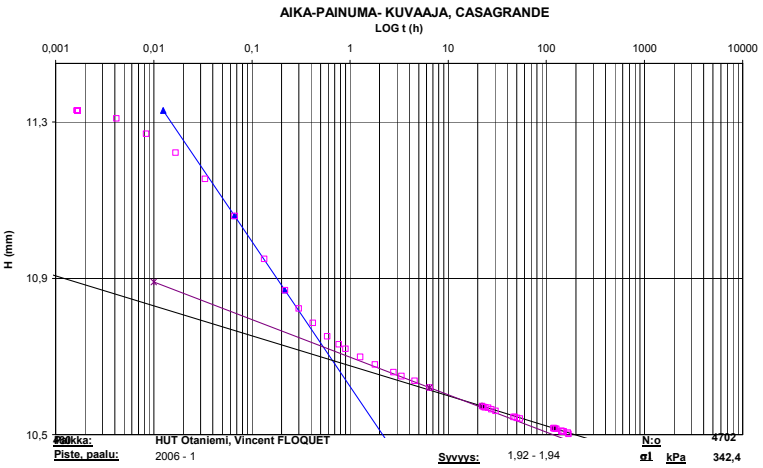

Figure 4.16 C_α *slope, best fitted/corrected (Load step 342,4kPa)*

Such apparently tiny differences can be of importance when it deals with long term settlements. For the load step 42,8kPa, secondary consolidation strain is about 20%

bigger when plotted without correction after 100 hours of consolidation (eventually, for the simulation, μ^* has been set to 2,95.E-3).

4.2.1.1.2 Results

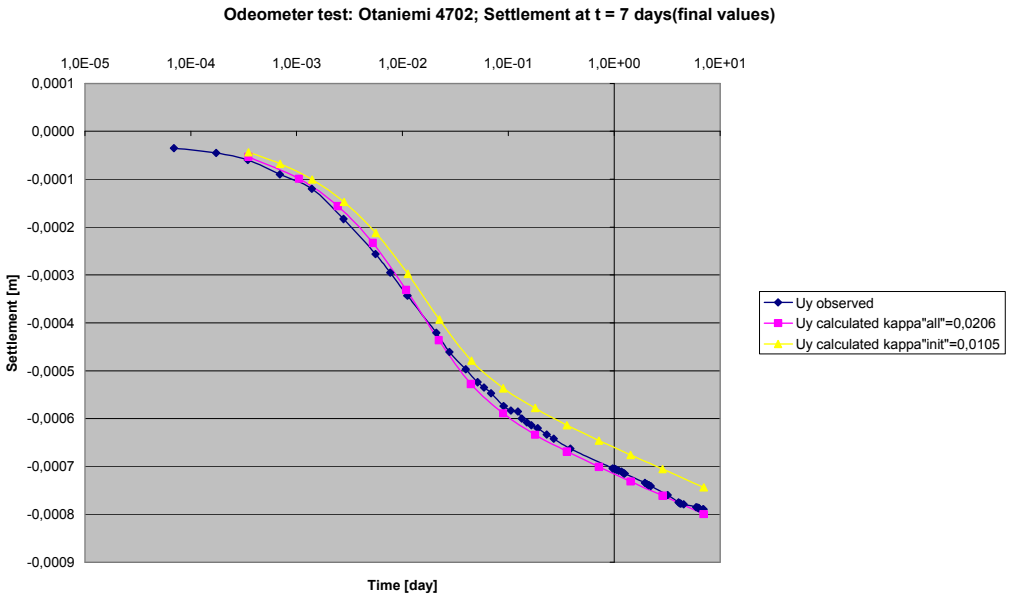

Figure 4.17 Computed/observed settlement of the 4702 oedometer test's sample λ (values at 7days) and κ obtained as described above

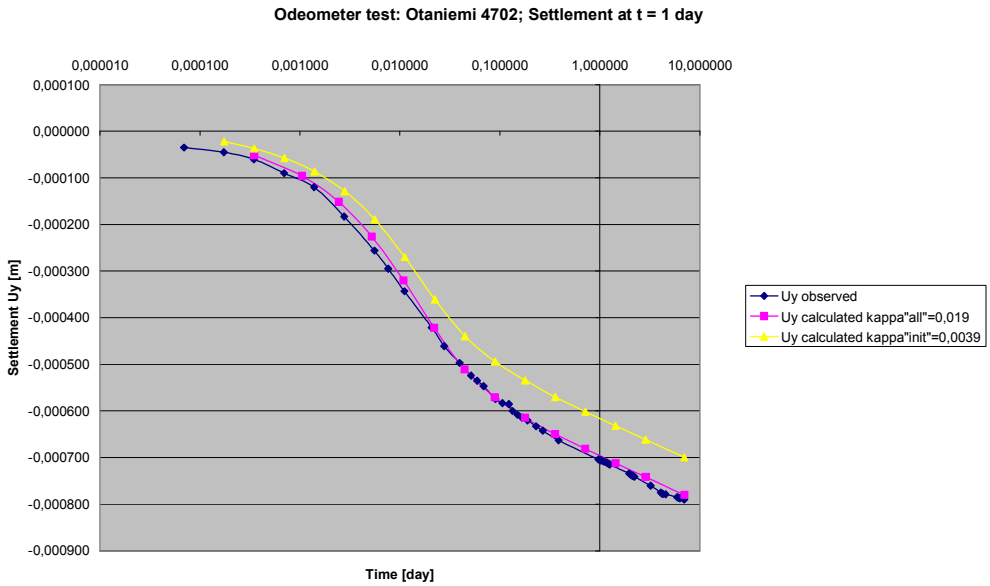

Figure 4.18 Computed/observed settlement of the 4702 oedometer test's sample λ (values at 1day) and κ obtained as described above

Figure 4.19 Computed/observed settlement of the 4702 oedometer test's sample / λ (values at 1/10day) and κ obtained as described above

If we compare now the difference in the calculated curves obtained with the different value of λ (values acquired by plotting the reading of the settlement at t=7days, t=1day and t=2,4H) we can notice that the difference between those curves is not noteworthy.

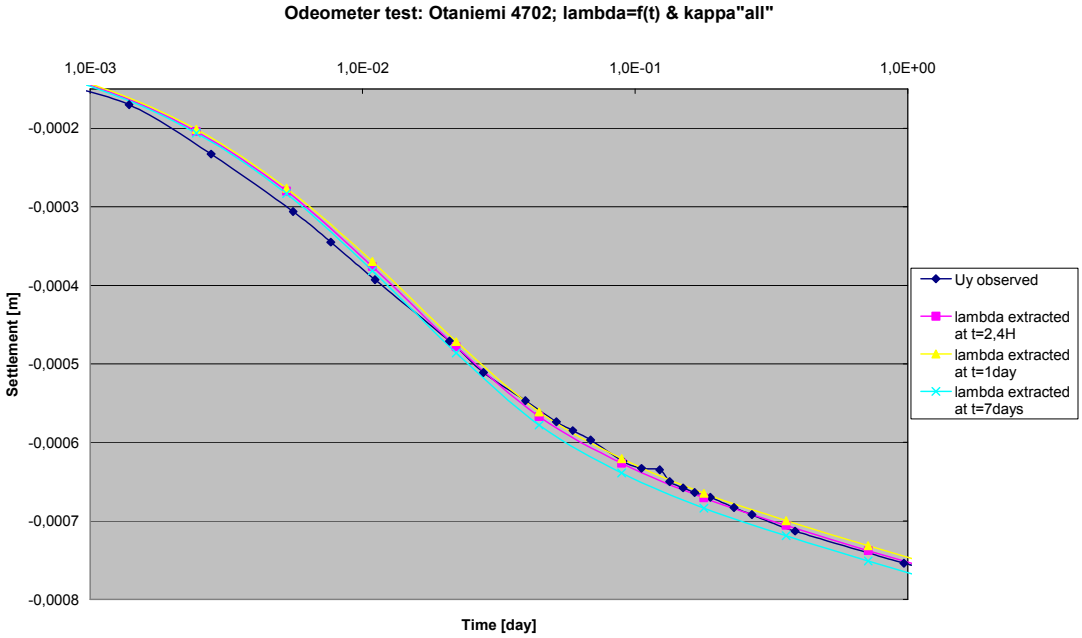

Figure 4.20 Comparison between the computed settlement of the 4702 oedometer test's sample; $\kappa = cst$, λ function of acquisition day values

Comments:

- Lambda values depends slightly on the time acquisition of the settlement values as we have seen but one should notice that these values are much more affected by the points used to get the lambda value from the experimental test results.
- The real value of kappa is hard to determine as it's not the only parameter which might be discussed in the modelling. One can suppose that the most correct value is situated between $\kappa_{"all"}$ and $\kappa_{"init"}$. Anyway as we have said before the curve is modelled by a straight line in this model which let us think that there's no absolutely right value.
- The values of the preconsolidation pressure and the permeability have been set in order to chock the model and stick as close as possible to the reality. The chocking has anyway not been exposed as it has not been subject to study. The range was given for the permeability by the Taylor's and Casagrande's assessment of the value [2,29.E-5m/day ; 3,65.E-5m/day]. For the preconsolidation pressure the range was given thanks to the different time acquisition curves: [24kPa ; 31kPa].

4.2.1.2 Otaniemi 806

4.2.1.2.1 Parameters

- Dimensions of the sample:
  - H_{init} =20 mm
  - A = 2000 mm^2

- $\sigma_1 = \sigma$ applied = 25 kPa
- $\sigma_{10} = \sigma$ applied at the previous load step = 12,5 kPa
- h_0 = height of the sample at the end of the previous load step = 19,361 mm

- λ^* = 0,24257
- κ^* = 1,0197.E-2
- μ^* =9,728.E-3
- k = 3,162.E-5 m/day

- e_0 = 3,6
- $POP = \left|\sigma_p - \sigma_{yy}^{'0}\right| = \left|12{,}5 - 0\right| = 12{,}5kPa$

- c = 2 kPa
- φ = 24˚
- ψ = 0˚

- γ_{sat} = 13,6 kN/m^3
- γ_{unsat} = 5,935 kN/m^3

4.2.1.2.2 Results

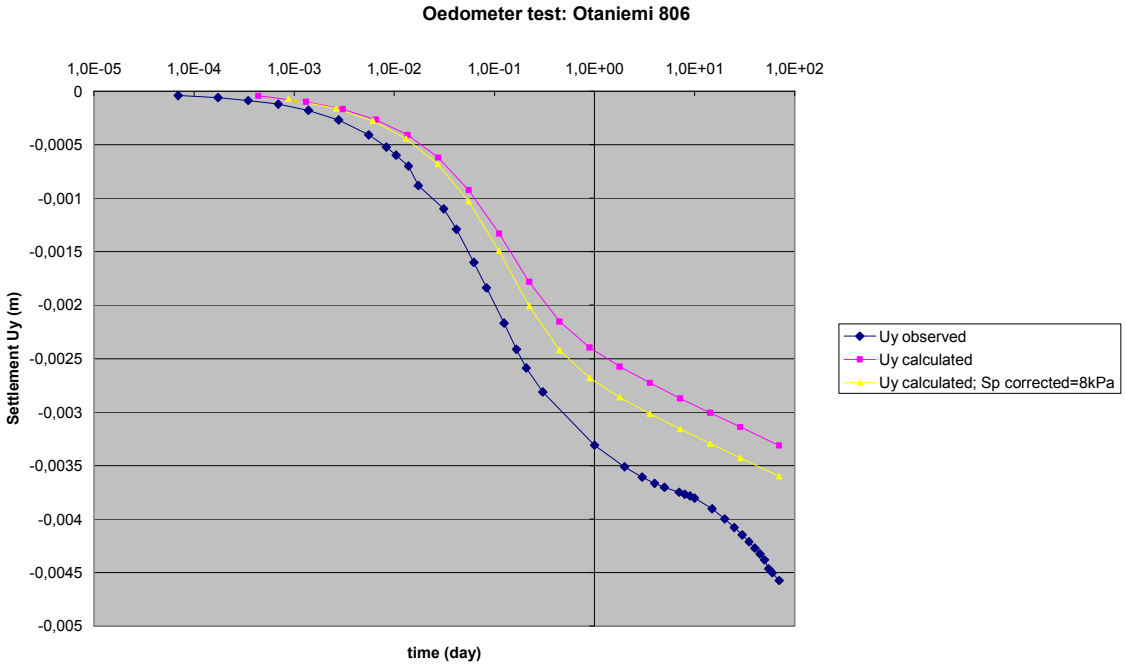

Figure 4.21 Computed/observed settlement of the 806 oedometer test's sample

Observations:

- The second part of the slope (λ*) seems to be acceptable (slope as steep as the slope observed)
- The end of primary consolidation seems a little bit delayed actually.
- The last part of the curve characterized by an increase of the slope is not taken into account in the PLAXIS Soft-Soil-Creep model.

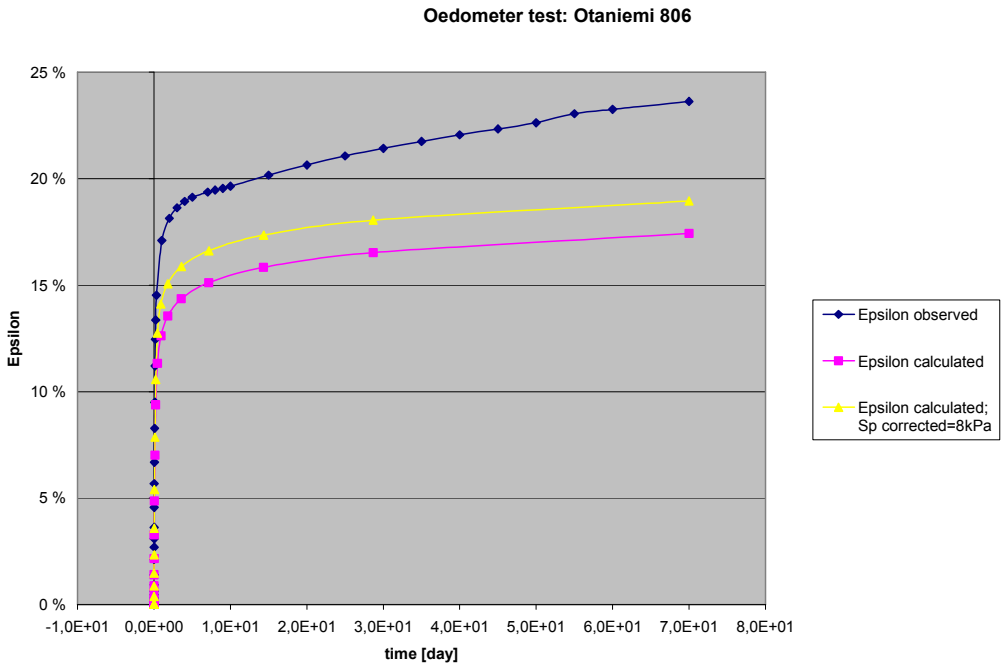

Figure 4.22 Computed/observed strain of the 806 oedometer test's sample

Error at 70 days [%] 27,6

Note that, the actual slope change makes this error grow consequently with time.

About the interest of plotting the curve Epsilon-time:

The height of the sample can't be settled in the simulation at the accurate value of 19,361mm. As the value assigned is 19 mm the settlement obtained is thus very close but not exactly the same as for a sample of 19,361mm high. The relative value Epsilon enables us to keep apart this source of error.

N.B: Here are presented the results of this two oedometer tests. Simulation of the other oedometer tests can be found in the Appendix 3.

Appendix 3: Taasia 21D1
Taasia 26B1
Vanttila 4452
Vanttila 4453
Perno 116
Suurpelto 4532
Suurpelto 4533

4.3 Analysis

What kind of clay behavior can we simulate with PLAXIS model:

Table 4.5 Validity of PLAXIS' Soft-Soil-Creep Model for the different tests

Test	Instant compression	Part of the curve modelling primary consolidation	Part of the curve modelling creep	Change in the slope of creep (increasing C_α)	Final error acceptable	Can be simulated with plaxis soft soil model
Otaniemi 806	1	2	3	YES	NO	NO
Taasia 21D1	1	1	1	NO	NO	YES
Taasia 26B1	1	1	1	NO	YES	YES
Vanttila 4452	1	1	1	NO	YES	YES
Vanttila 4453	1	1	1	YES	YES	YES
Perno 116	1	1	1	YES	NO	-
Suurpelto 4532	1	1	1	YES	NO	NO
Suurpelto 4533	3	3	2	NO	NO	NO
Otaniemi 4702	1	1	1	NO	YES	YES

(1) good accuracy of the model, stick to actual behavior

(2) different but acceptable

(3) non acceptable

One can note that all the tests can't be simulated properly thanks to PLAXIS model. For those that can't be simulated, one should get back to classical modelling.

5 CLASSICAL MODELLING OF OEDOMETER TESTS

5.1 The Asoaka method (1978)

Asaoka method is a method to determine the ultimate primary consolidation. The biggest advantage of the method is its simplicity. Indeed no soil properties are required to determine with this method the ultimate primary consolidation /Stapelfeldt 2000/.

Asaoka admitted that one-dimensional consolidation settlements at certain time intervals could be described as a first order approximation:

$$S_n = \beta_0 + \beta_1 S_{n-1} \tag{5.1}$$

Where S_n is the time settlement at time t_n. The time interval $\Delta t = (t_n - t_{n-1})$ is constant.

The first order approximation should represent a straight line on a (S_n vs. S_{n-1}) co-ordinate. The values of β_0 and β_1 are given by the intercept of the fitted straight line with the S_n-axis and the slope.

The ultimate primary settlement can be calculated thanks to the expression:

$$S_{ult} = \frac{\beta_0}{1 - \beta_1} \tag{5.2}$$

This value is so determined graphically by the intercepting point with 45°-line i.e. when $S_n = S_{n-1}$.

N.B 1: This method assumes that the soil is homogeneous and the load constant.

N.B 2: To get a correct line it is of major importance to use points of primary consolidation. (points of instant compression and secondary compression are proscribed)

N.B 3: Tan and Chew (1996) exposed in their article that estimation of the ultimate primary consolidation may be corrected depending on the data used to plot the curve (time of consolidation) /Holtz 1991/.

Table 5.1 Validity and correction of the results obtained thanks to Asaoka method

	Estimation of S_{ult}	**Estimation of c_v**
Data 0-30% of consolidation	underestimated	overestimated
Data 30-60% of consolidation	Underestimated (10%)	Overestimated (30%)
Data >60% of consolidation	Exact value	Exact value

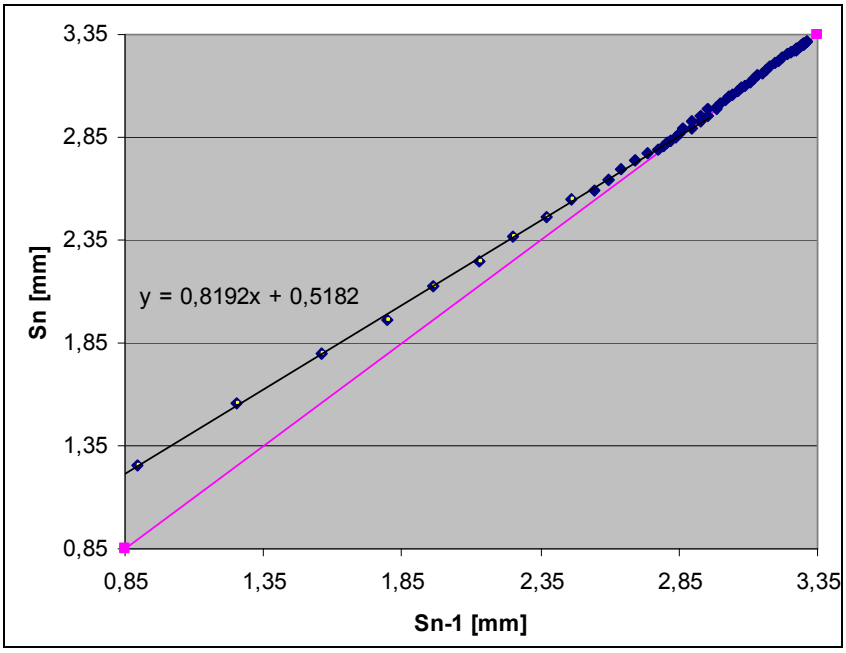

Fig 5.1 Otaniemi 806: Asaoka method Δt=0,5 h

β0	0,5182
β1	0,8192
Sult [mm]	2,86615

Consolidation: U[%] = 63,23%

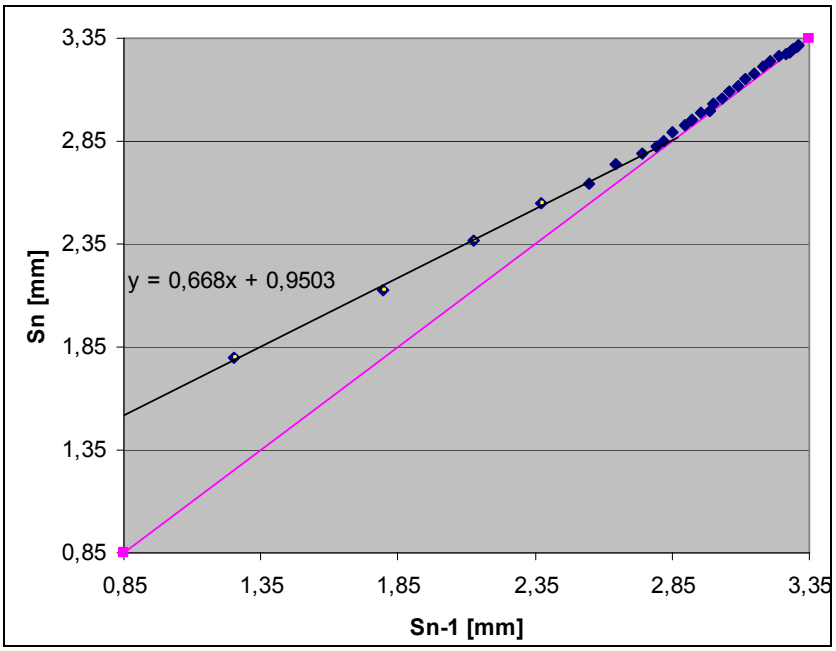

Fig 5.2 Asaoka method Δt=1 h

β0	0,9503
β1	0,668
Sult [mm]	2,862349

Consolidation: U[%] = 63,14%

5.2 The hyperbolic model

This method first proposed by Korhonen (1977) and then improved by Puumalainen (1998) includes modelling of primary and secondary settlement /Stapelfeldt 2000/.

It assumed that the settlement speed is reduced in a hyperbolic manner /Länsivaara/, the time/settlement curve is given as:

$$S = \frac{t}{\frac{1}{v_0} + \frac{t}{S_f}} \tag{5.3}$$

Where

	t	time
	S	settlement at time t
	S_f	final predicted settlement (= S_{ult} + S_s)
	S_{ult}	ultimate primary settlement
	S_s	secondary settlement
	V_0	settlement speed at start of observations (t=0)

This equation can be written this way:

$$\frac{t}{S} = \frac{1}{v_0} + \frac{t}{S_f} \tag{5.4}$$

Thus on the (time/settlement vs time co-ordinate) the inverse of the slope of the straight line denotes the final predicted settlement, S_f, and the interception with time/settlement axis denotes the value $1/v_0$.

N.B: This method assumes as for the Asaoka method that the soil is homogeneous and the load constant.

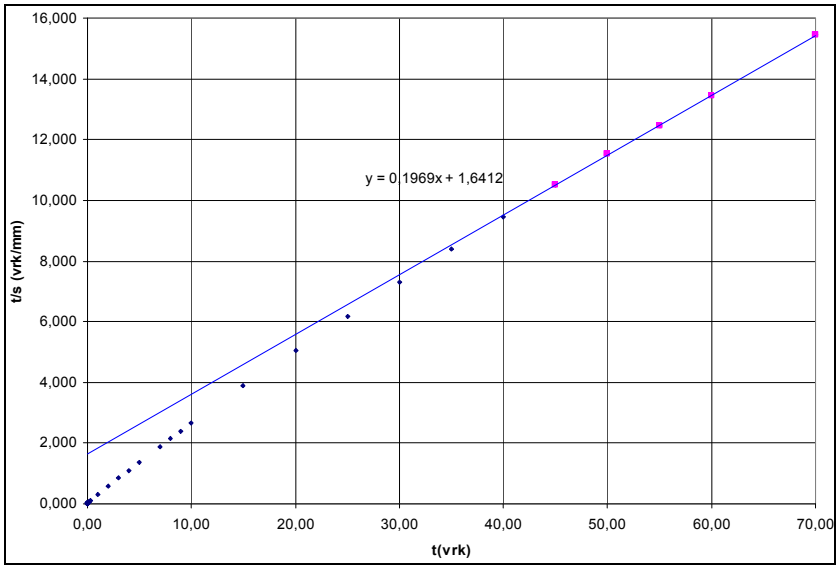

Fig 5.3 Otaniemi 806: Determination of the hyperbolic model parameters

v_0 [mm/day]	0,609
S_f [mm]	5,08

The problem with this parameter is that the simulation is not that accurate if we compare to what happen actually. To make it with this we can divide the curve in two parts and assess the parameters for the two parts of the curve with the same method.

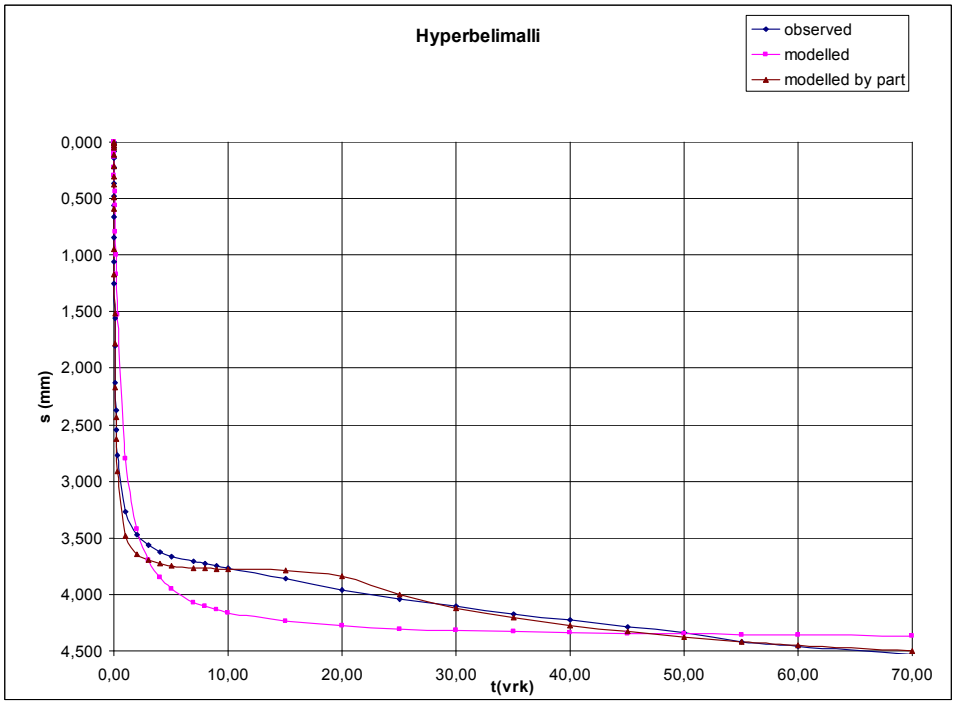

Fig 5.4 Hyperbolic model of Otaniemi 806 oedometer test

5.3 The Buisman model

To predict the settlement Buisman method uses the classical parameter describing secondary compression as explained in chapter 2 /Perrone 1998/.

The settlement is thus calculated from the formula 5.5 below and required to know parameter like the coefficient α_s that we are supposed to extract from experimental results /Vermeer/.

$$S = H_{EOP}.\alpha_S.\Delta\log(t) \tag{5.5}$$

Where
- t — time
- S — settlement at time t
- H_{EOP} — height of the sample at the end of primary consolidation
- α_s — coefficient of secondary compression

But this formula is only of use to calculate the secondary compression. One must add the settlement due to primary consolidation. This is made thanks to Brinch-Hansen method.

This method uses this formula (5.6) to assess the settlement:

$$\frac{S}{S_p} = \sqrt[6]{\frac{t^3}{t_{90}^3 + t^3}} \tag{5.6}$$

Where
- S — settlement at time t
- S_p — settlement at the end of the primary consolidation
- t — time
- t_{90} — time at 90% of the primary consolidation

The value of the t_{90} and S_p are assessed thanks to Taylor's method (c.f chapter 3).
Thus the height of the sample is:

$$H = H_0 - S_p \sqrt[6]{\frac{t^3}{t_{90}^3 + t^3}} - \begin{vmatrix} 0 \Leftarrow t < t_{EOP} \\ H_{EOP}.\alpha_s.\Delta\log(t) \Leftarrow t \geq t_{EOP} \end{vmatrix} \quad (5.7)$$

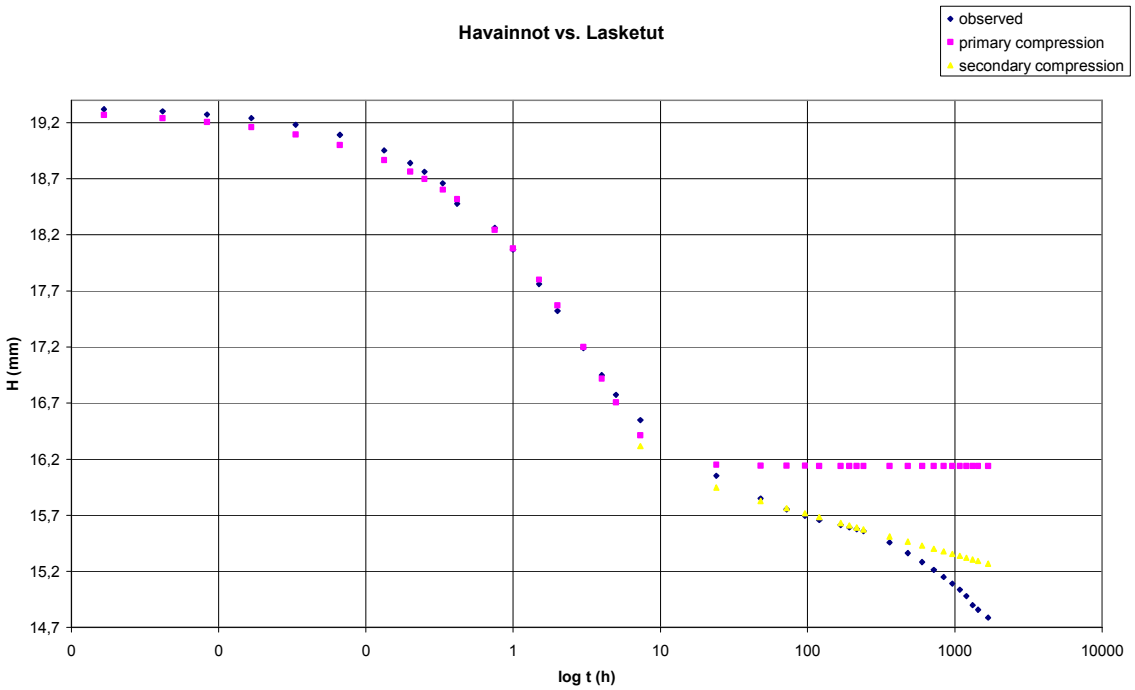

Fig 5.5 Otaniemi 806: Buisman (/Brinch-Hansen) model

But with this modelling one can notice that the second part of the secondary compression is not modelled. That's why another model for clay with such behavior is used, a model considering this phenomenon.

5.4 Anagnosti model

As for Buisman model Anagnosti's model has been developed to predict settlement due to secondary compression. The primary settlement will therefore be modelled thanks to Brinch-Hansen model (c.f chapter Buisman model).

Anagnosti's equation:
The model is based on Kelvin's and Maxwell's way of modelling the soil (parallel and serie spring/dashpot system) /Tanska 1993/, which enable to extract equation below:

$$3K_0\nu_d\frac{d\varepsilon_z}{dt}+\left(3\nu_0\nu_d+\frac{3K_0\nu_d^2}{G}\right)\frac{d^2\varepsilon_z}{dt^2}+\frac{3\nu_0\nu_d^2}{G}\frac{d^3\varepsilon_z}{dt^3}=2K_0\left(\sigma_z-\sigma_r\right) \tag{5.8}$$

Where
- K_0 bulk compressibility modulus
- ν_0 coefficient of bulk viscosity
- ν_d coefficient of deviatoric viscosity
- G rigidity modulus
- ε_z vertical strain
- σ_z axial stress
- σ_r radial stress

The solution of which is /Anagnosti 1963/:

$$\varepsilon_z=C_{1V}e^{-\frac{K_0}{\nu_0}t}+C_{2V}e^{-\frac{G}{\nu_d}t}+C_{3V} \tag{5.9}$$

With C_{1V}, C_{2V}, C_{3V} Volume changing constant

Determination of the parameters

- K_0

$$K_0=\frac{\sigma_z+2\sigma_r}{3\varepsilon_{zfl}} \quad \text{with} \quad \varepsilon_{zfl}=\varepsilon_{zf}+\varepsilon_{zc} \tag{5.10}$$

Where ε_{zfl} strain due to secondary consolidation

ε_{zc} strain due to primary consolidation

ε_{zf} total strain

ε_{zc} is determined thanks to Taylor's method (strain at 100% of the consolidation). Concerning ε_{zf} the best way to assess it, is to plot the t/Epsilon-t chart and to determine the slope of the final part of the curve.

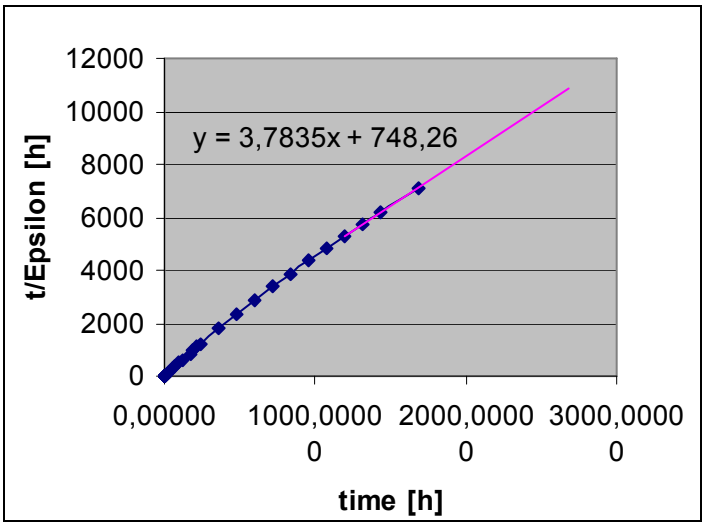

Fig 5.6 t/ε-t diagram: Otaniemi 806 oedometer test; $\varepsilon_{zf} = 1/3{,}7835 = 0{,}264$

- $\frac{G}{\nu_d}$ and C_{2V}

By calculating the limits of Anagnosti's solution we can write:

$$\ln(A) = \ln\left(\frac{\sigma_z + 2\sigma_r}{3K_0} - (\varepsilon_z - \varepsilon_{zc})\right) = \ln(-C_{2V}) - \frac{G}{\nu_d}t \qquad (5.11)$$

We can therefore obtained C_{2V} and $\frac{G}{\nu_d}$ by plotting the lnA-t diagram and then assessing the slope and axis intercept of the line modelling the last part of the curve:

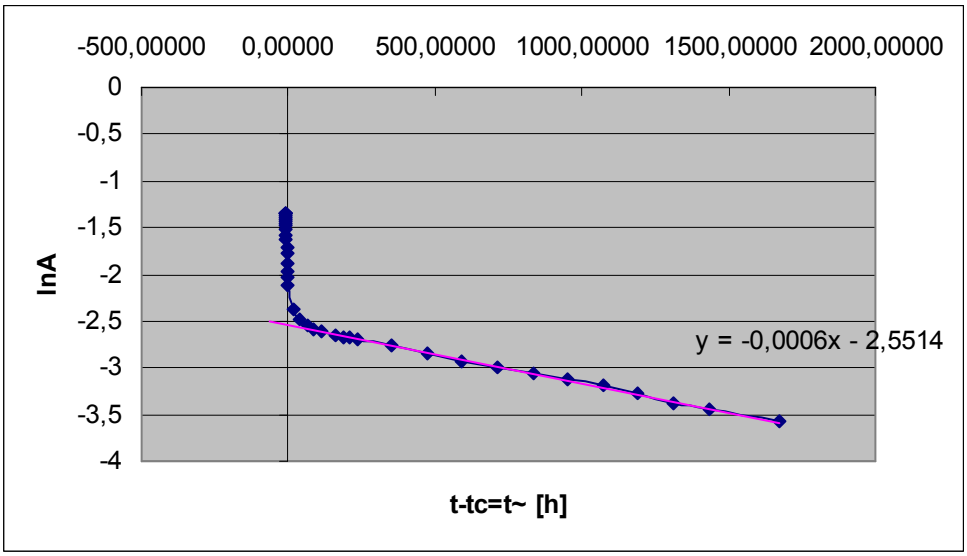

Fig 5.7 Otaniemi 806, lnA-t~: $C_{2V} = -e^{-2,5514} = -0,07797$; $\frac{G}{\nu_d} = -0,0006$

- C_{1V}

C_{1V} is easily calculated once C_{2V} obtained thanks to this formula resulting from boundary consideration on Anagnosti's solution:

$$C_{1V} = -C_{2V} - \frac{\sigma_z + 2\sigma_r}{3K_0} \tag{5.12}$$

- ν_0

Let's still consider boundary values ($t \to 0$), then ν_0 can be calculated as described below:

$$\nu_0 = \frac{K_0 C_{1V}}{\dot{\varepsilon}_v(t=0) + \frac{G}{\nu_d} C_{2V}} \tag{5.13}$$

For example for Otaniemi 806:

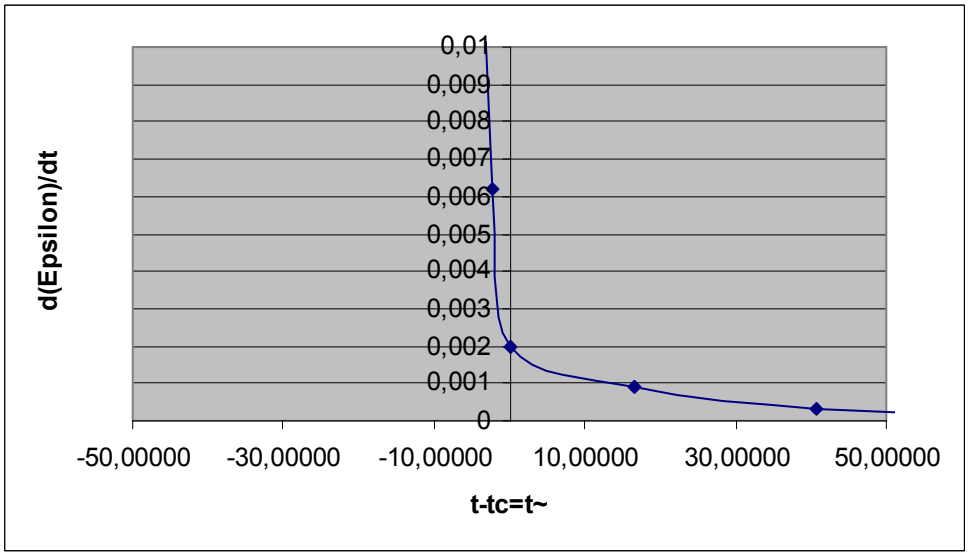

Fig 5.8 Otaniemi 806, dε/dt-t~: $\dot{\varepsilon}_v(t=0) = 0{,}001963 \Rightarrow \nu_0 = 3212{,}43$ kPah

$\dot{\varepsilon}_v(t=0) = 0{,}001963$ and so $\nu_0 = 3212{,}43$ kPah

N.B:

Acquiring of this parameter is not that reliable and is of great influence on the shape of the predicted curve. Indeed $\dot{\varepsilon}_v(t=0)$ can be from simple to double value (changing at the same time the value of ν_0) depending on the points used for calculation of the Volume changing rate ((t-1;t); (t;t+1); (t-1;t+1)). This modifies consequently the shape of the curve.

- $C_{3V} = \dfrac{\sigma_z + 2\sigma_r}{3K_0}$ (5.14)

All the necessary parameters are now known. We can plot the value of the observed and calculated strain (with Anagnosti's model eq 5.15):

Table 5.2 Parameters for the Anagnosti/Brinch-Hansen modelling

Parameter's to Brinch-Hansen's equation		
ε_{EOP} =15,753%	t_v =6,54 h	c_v =0,09 m^2.a^{-1}
Parameter's to Anagnosti's equation		
K_0 =149,77 kPa	C_{1V} =-0,04109 h	ε_{zc} =14,52%
ν_0 =3212,43 kPa.h	C_{2V} =-0,07797 h	ε_{zf} =26,43%
$\frac{G}{\nu_d}$ =0,0006 h^{-1}		

$$\varepsilon = \begin{cases} \varepsilon_{EOP} \cdot \sqrt[6]{\frac{t^3}{t_{90}^3 + t^3}} \Leftarrow if\ .t < t_{EOP} \\ C_{1V} e^{-\frac{K_0}{\nu_0} t} + C_{2V} e^{-\frac{G}{\nu_d} t} + C_{3V} \Leftarrow if\ .t \geq t_{EOP} \end{cases} \qquad (5.15)$$

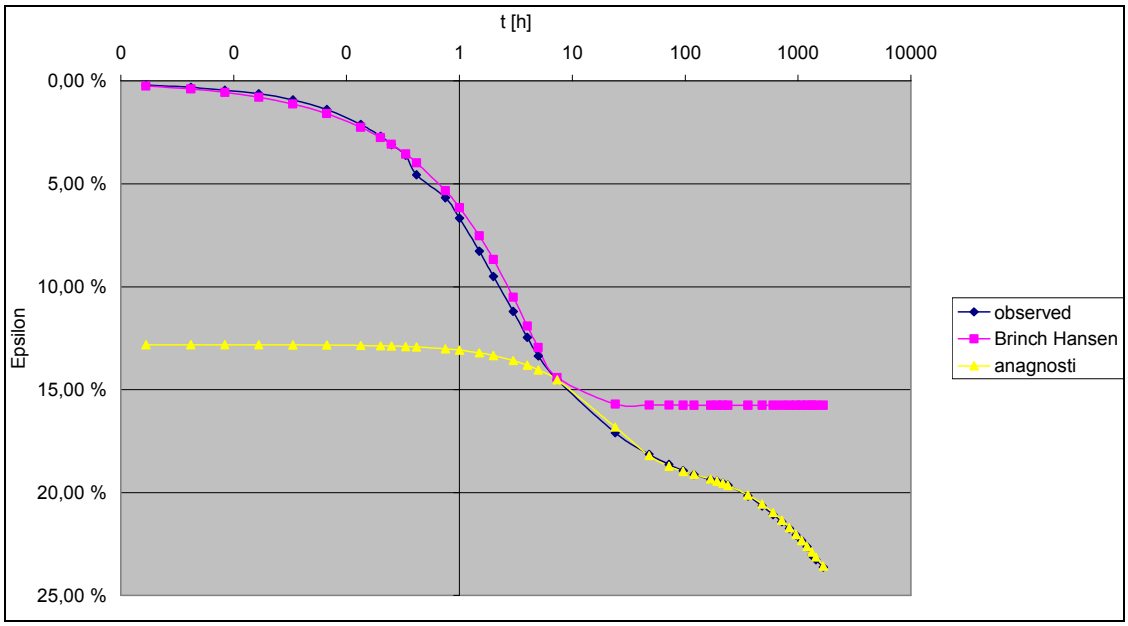

Fig 5.9 Otaniemi 806: Brinch-Hansen model; Anagnosti model

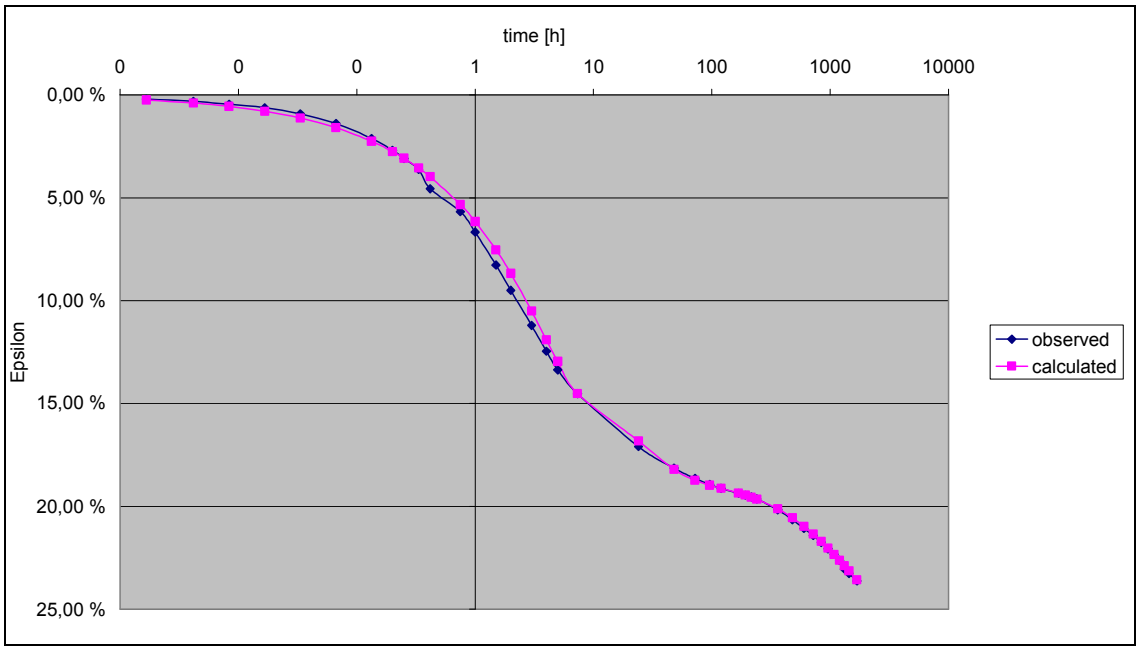

Fig 5.10 Otaniemi 806: Brinch-Hansen/Anagnosti model

Anagnosti's model is, thanks to its accuracy for this particular clay behavior, probably the fittest model to predict settlements. The second part of secondary compression is regarded.

6 CONCLUSION

The aim of this final project was to study the different model and way to model the creep behavior of soft Finnish clay. As a support, oedometer test Otaniemi 806 and Otaniemi 4702 has been processed in this work. They deliver the advantage of showing two different behaviors occurring during secondary consolidation. All along my work here, Test Otaniemi 4702 has been carried out from sampling on the field to the final stage of the oedometer test which has given me an overall view of the laboratory work. Other tests have nevertheless been studied (not as deep as for these one) and can be found attached in appendices.

Plaxis Soft-Soil-Creep model has shown its limits using strictly Buisman model. The way of modelling has been checked and is apparently correct. One can therefore come to the conclusion that the problem comes from the model itself (Buisman model) which doesn't fit to certain particular clay, e.g. Otaniemi 806. Indeed we expected this insufficiency of the model regarding the equation and the parameter describing the model (linear law with logarithm of time for settlement due to secondary compression).

Otaniemi 806 oedometer test has thus been modelled properly thanks to a classical model with Excel software. Anagnosti's model has proved here a good accuracy. It achieves to model properly clay the behavior of which shows a second phase (increase of settlement's rate) in secondary compression. It should supersede Buisman model in this way that Buisman model simulate settlement due to secondary consolidation of clay in proportion with logarithm of time.

But classical modelling has not proved to be always necessary and many clays behavior can be modelled accurately enough with PLAXIS Soft-Soil-Creep model. Anyway results got from PLAXIS simulation should be considered in hindsight. The different assumptions and the scale of the sample simulated could also influence the results, when applied to bigger scale problems.

Study about getting parameters from the test the most properly has also proved interest. However the first point to consider is using a fitted model, the accuracy and cares about objective acquiring of parameters should only then be regarded. On this point no particular method could be advisable but those that seems first to be correct according to the observer. That's why, it should be advised to set parameters the values of which

are not that influenced by the way to work them out and make vary, in the assessed range, one parameter after another to chock the model to the actual behavior. Trying to put in practise the different theories and assumptions formerly enunciated (e.g. Mesri) should be considered in the second instance and cautiously.

It could have been interesting to regard how temperature influences the results as it should play a role of importance in Finland. A study about the scale effect and under which conditions parameters could be considered as correct at larger scale, in the construction site, could have also brought useful information.

REFERENCES

Aalto.A & Lojander.M & Ravaska.O (2004), *"*On the stress-dependence of settlement parameters of Finnish clays", *Proc. of XIV Nordic Geotechnical meeting,* Swedish Geotechnical Institute*, Vol.2 I-27.*

American Society for Testing and Materials (1985), *Classification of Soils for Engineering Purposes: Annual Book of ASTM Standards*.

Anagnosti Dr.-Ing Petar (1963), *Stresses, deformations and pore pressure in triaxial test obtained by a suitable rheological model*, Beograd, Yugoslavia.

Bjerrum.L (1974), *Publication Nr.100 – Problems of Soil Mechanics and Construction on Soft Clays*, Norwegian Geotechnical Institute, Oslo.

Claesson. P (2003), *Long term settlements in soft clays*, Department of geotechnical engineering, Chalmers University of technology, Goteborg, chapter 2.

Hiroshi Yoshikuni and Osamu Kusakabe (1995), *Compression and consolidation of clayey soils*, Department of Civil engineering, Hiroshima University, Japan, p.720.

Holtz R.D, Jamiolkowski M.B, R Lancellotta, R Pedroni (1991), *Prefabricated vertical drains: design and performance*, University of Washington- Politecnico di Torino, chapter 5.9.

Ian K. Lee / Weeks White / Owen G.Ingles (1983), *Geotechnical engineering*, University of New South Wales, Australia, chapter.5.

Länsivaara T.T, *Observational approach for settlement predictions*, Tampere University of Technology, Finland.

Larsson.R (1986), *Consolidation of soft soils - Report 29*, Swedish Geotechnical Institute, Linköping.

Larsson.R, Bengtsson P-E, Eriksson L (1997), *Prediction of settlements of embankments on soft, fine-grained soils. Calculation of settlements and their course with time*. Swedish Geotechnical institute, Linköping.

Standard ISO/TS 17892-5:2004, Geotechnical investigation and testing -- Laboratory testing of soil -- Part 5: Incremental loading oedometer test.

Tanska.H (1993), *Master's thesis - Suljetun leikkauslujuuden kasvu primaarisen ja sekundaarisen konsolidaation aikana*, Helsinki University of Technology.

Perrone Vincent.J (1998), *One dimensional computer analysis of simultaneous consolidation and creep of clay,* Virginia polytechnic institute, Blacksburg, chapter 2.

PLAXIS version 8, Material models manual.

Pusch. R (1978),"Creep mechanisms in clay", *Proc. of Mechanisms of deformation and fracture*, University of Luleå, Sweden, Vol.1: p.292.

Stapelfeldt Timo (2000), *Special assignment - Observational method for settlement prediction*, Helsinki University of Technology, Helsinki.

Svanø.G & Christensen.C (1991), *A soil model for consolidation and creep*, The Norwegian Institute of Technology, Norway.

Vermeer P.A & Neher H.P, *A soft soil model that accounts for creep*, Institute of Geotechnical Engineering, University of Stuttgart, Germany.

APPENDIX 1 (additional theoretical consideration)

The relationship between effective stress, strain and strain rate

In 1985 Leroueil et al. conducted a comprehensive study of different tests on various types of clays with the objective of determining the rehological behavior of soft clays. They proposed that the rehological behavior of one-dimensional consolidation of clays is controlled by a unique relationship between stress, strain and strain rate (σ'-ε-$\dot{\varepsilon}$). This relationship can be described by just two functions. The first gives the relationship between preconsolidation pressure and the strain rate, equation (1'). The second relationship described the normalized effective stress-strain curve by means of equation (2'), see Figure 1:

$$\sigma'_p = f(\dot{\varepsilon}_v) \qquad (1')$$

$$\frac{\sigma'_v}{\sigma'_p} = g(\varepsilon_v) \qquad (2')$$

where σ'_p = consolidation pressure

σ'_v = vertical effective stress [kPa]

ε_v = vertical strain

$\dot{\varepsilon}_v$ = vertical strain rate [1/s]

$f(\dot{\varepsilon}_v)$ = a function of vertical strain rate

$g(\varepsilon_v)$ = a function of vertical strain

The rheological model is in line with the model including sets of isotaches proposed by Suklje (1957).

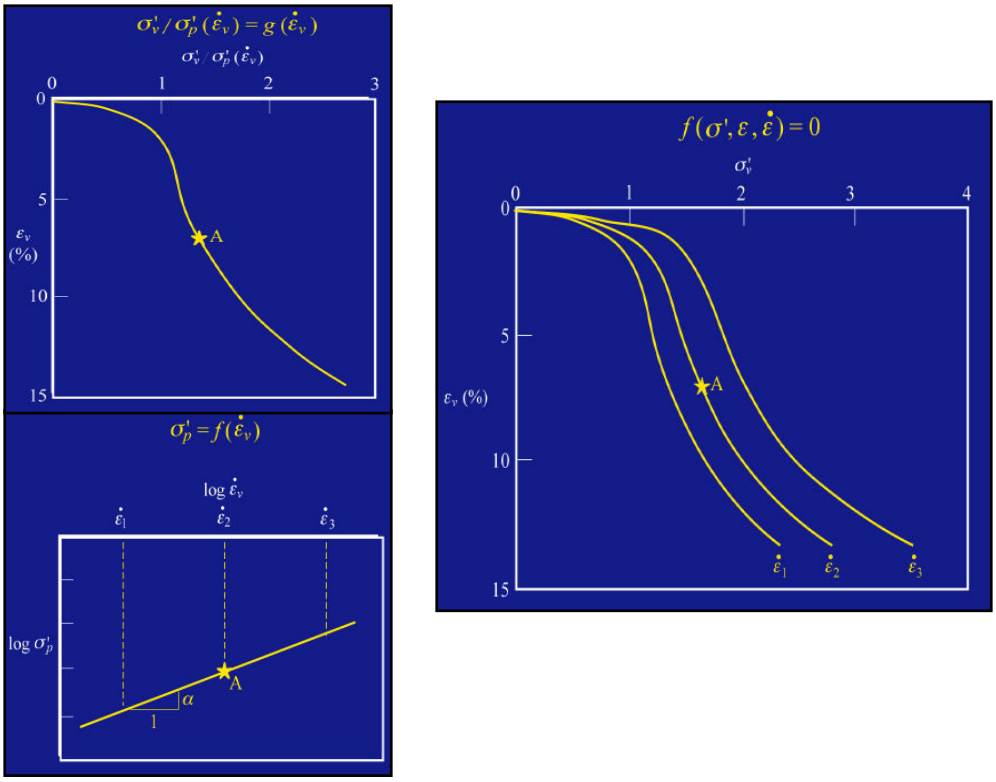

Figure 1' Suggested model for natural clays (Leroueil et al., 1985)

The observation that the preconsolidation pressure is dependent on the strain rate has been recognized by many researchers, e.g. Sällfors (1975), Larsson (1981), Graham et al. (1983) and Leroueil et al. (1985) to mention but a few. This behavior can be exemplified by CRS-tests with different strain rates.

In Figure 2' another important test result (Mesri et al 1995) is presented, which confirms the behavior described. For a 500mm long sample the effective stress – strain curves of four different sub-layers were monitored. The stress-strain curves vary, depending on the distance of each sub-element to the drainage boundary. For sub-element 1, close the drainage surface, the strain rate is higher than in other sub-elements. The resulting effect is that, for a higher strain rate, a higher magnitude of effective stress was obtained in the initial branch of the curve, i.e. the apparent preconsolidation pressure increased. Analogous results were also reported by Berre and Iversen (1972). Moreover, the results presented in Figure 2.9 show clearly how the consolidation process and the apparent preconsolidation pressure vary in the clay strata due to different drainage conditions.

It can also be noted that the point of EOP, in Fig 2', seems to be equal of all sub-elements. Mesri and Choi (1985) proposed that there is a unique EOP e- logσ' curve for any soft clay. This statement is not in line with e.g. Suklje (1957), Berre and Iversen (1972) and Yin and Graham (1996), who concluded that the relationship between strain and effective stress at the EOP depends on the thickness of the clay specimen/layer.

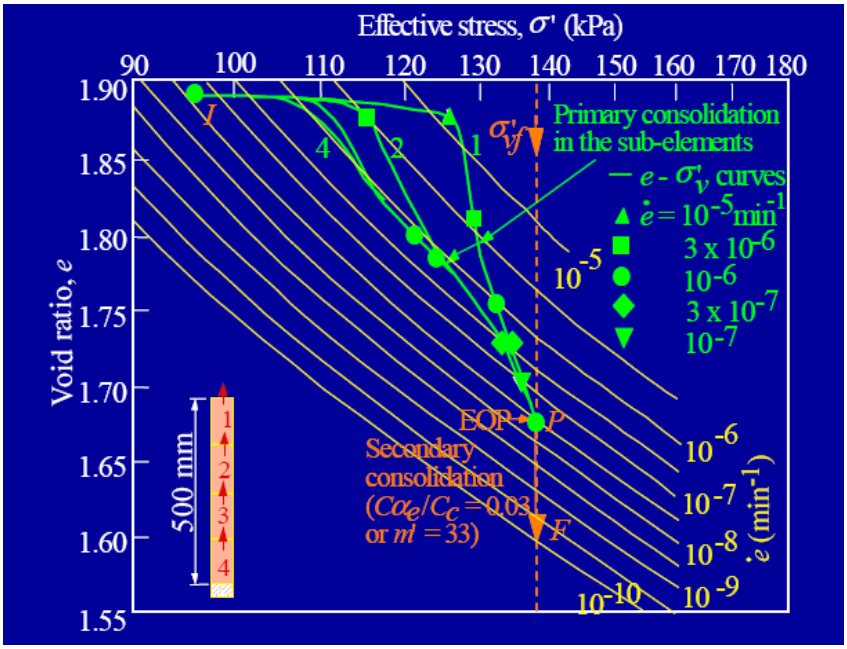

Figure 2' *Consolidation of St-Hilaire clay for pressure increment from 97 to 138 kPa (results from Mesri and al. (1995), reinterpreted and presented by Leroueil and Marques, 1996).* C_α*, secondary compression index;* C_c *compression index;* $\dot{e}$ *rate of void ratio and* $m' = C_c / C_\alpha$.

In 2001 Leroueil and Kim proposed a non-linear viscoplatic model for one-dimensional consolidation, where the strain is divided into two parts: elastic strains and the viscoplastic strains. This model is a further development of the model presented by Leroueil and al. (1985).

The effect of temperature on the compressibility

The behavior of natural clay during consolidation is evidently not influenced only by the strain rate. Temperature is also an important factor, especially in the normally consolidated range and also in terms of the magnitude of the preconsolidation pressure. The influence of temperature on the compressibility of natural clays has been investigated by authors such as for example Sällfors (1989) and Boudali and al. (1994). In 1994, Boudali and al. proposed a generalization of the model suggested by Leroueil (1985), which takes the temperature into consideration.

Tidfors and Sällfors (1989) found that if the temperature increased from about +7°C, which is the normal temperature in-situ, to about 20°C, the preconsolidation pressure for a high plastic clay decreases with 6 to 10%. Leroueil and Marques (1996) obtained results that were in agreement with that.

However, the temperature in a clay deposit is normally constant and the temperature effects can be neglected in this work.

Determination of the creep parameter from CRS tests

Länsivaara (1995, 1999) proposed a model that made it possible to determine the creep parameter *time resistance number*, r_s, from CRS tests with different strain rates. However the model assumed that the compression modulus increases linearly with effective stress. For Swedish clays the compression modulus is evaluated as constant from σ'_c to σ'_L . This implies that the relation becomes more complex and thus more difficult to solve. Länsivaara utilized the unique relation between preconsolidation pressure and effective stress at a given strain (see equations (1') and (2')) and derived:

$$\frac{\sigma'_{v1}}{\sigma'_{cv1}} = \frac{\sigma'_{v2}}{\sigma'_{cv2}} \qquad (3')$$

Where σ'_{v1} = the effective strain for the strain rate $\dot{\varepsilon}_1$

σ'_{cv1} = The preconsolidation pressure for the strain rate $\dot{\varepsilon}_1$

σ'_{v2} = effective stress for the strain rate $\dot{\varepsilon}_2$

σ'_{cv2} = the preconsolidation pressure for the strain rate $\dot{\varepsilon}_2$

In addition to the strain rate relation the equation can be expressed as (Länsivaara 1995):

$$\frac{\sigma'_{v1}}{\sigma'_{v2}} = \frac{\sigma'_{cv1}}{\sigma'_{cv2}} = \left(\frac{\dot{\varepsilon}_1}{\dot{\varepsilon}_2} \right)^B \qquad (4')$$

Where the parameter B was determined. Länsivaara proposed that parameter B is equal to equation (2.19), i.e.

$$B = \frac{m}{r_s} = \frac{C_\alpha}{C_c} \qquad (5')$$

Which describe the relation between the creep and primary compression parameters in the equation.

Hence the time resistance number can be determined from:

$$r_s = \frac{M(\sigma')}{\sigma'.B} \qquad (6')$$

Länsivaara (1999) found that the value of B for Finnish clays is about 0.073.

Leroueil and Kim (2001) suggested an elastic viscoplastic (EVP) model. The model utilizes the relationship between the preconsolidation pressure and strain rate to describe the viscous behavior. By conducting CRS tests with different strain rates, determining the preconsolidation pressure at each strain rate and then plotting the results in a diagram as shown in Figure 3', thus making it possible to interpret a linear relationship between the plotted results. The equation describing the relation between

preconsolidation pressure and viscoplastic strain rate, $\sigma'_p = f(\dot{\varepsilon}_v^{vp})$, can be expressed as a linear function in a $\log\sigma'_p = \log\dot{\varepsilon}_v^{vp}$ diagram:

$$\log\sigma'_p = \Gamma + C_p.\log\dot{\varepsilon}_v^{vp} \qquad (7')$$

Where Γ = the value of log σ'_p at $\dot{\varepsilon}_v^{vp}$ =10^0 1/s

$\dot{\varepsilon}_v^{vp}$ = viscoplastic strain rate

$$C_p = \left(\frac{\partial \log\sigma'_p}{\partial \log \dot{\varepsilon}_v^{vp}} \right)$$

the preconsolidation index is denoted C_p and is equal to the value of C_α/C_c, which according to Mesri and Castro (1987) is between 0.03-0.05.

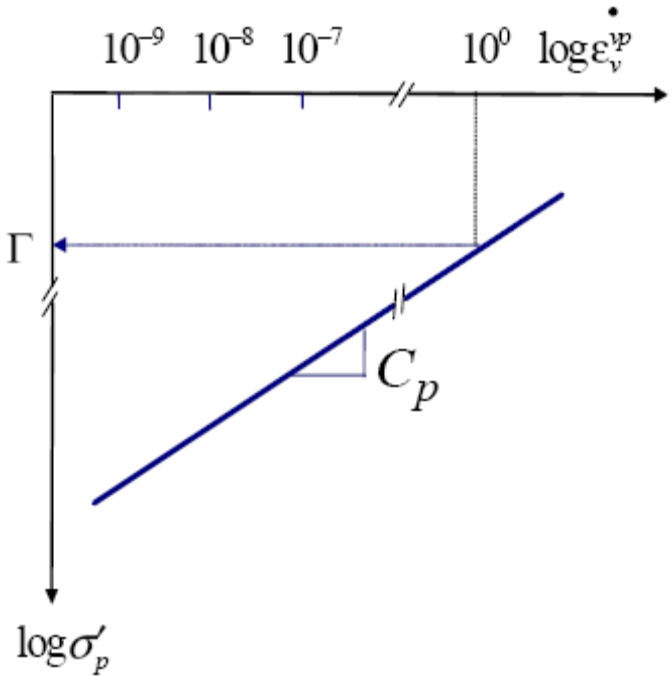

Figure 3' *Definition of the parameter C_p and Γ (Kim and Leroueil, 2001)*

These two parameters define the viscous behavior of the clay.

APPENDIX 2

Sampling

In order to carry out the tests, clay samples are taken from different sites in Finland. Here are some:

Perno (Turku)

Taasia

Otaniemi Vanttila (Espoo)

Figure 1" Different sampling sites

I have attended a course explaining in situ how to extract an undisturbed sample. The method consists in a first part of analysing the soil in place to know approximately the depth and thickness of the different layers. Then as we were interested in clay, a sample of this kind of soil at the chosen depth was extracted with the help of a standard piston sampler. To get the less disturbed sample as possible, avoiding vibrations is fundamental and hammer hits must be used as the worst solution. Here the stiffness of the soil was soft enough not to use predrilling. The sample was thus preserved in the piston sampler until its use in the laboratory.

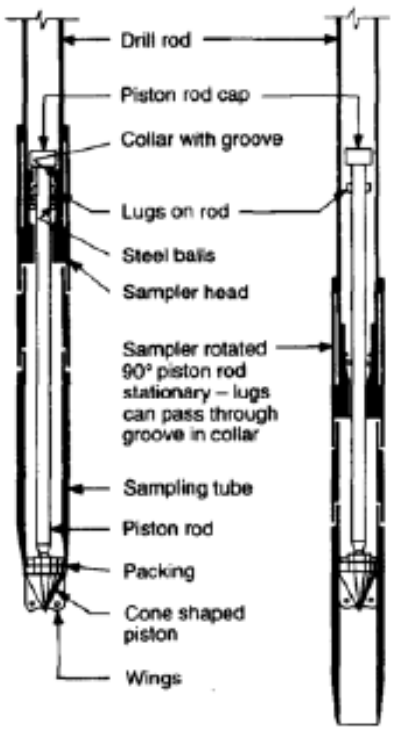

Figure 2" *Standard piston sampler*

Figure 3" *Weight sounding, soil layer identification*

Classification data

Criteria for distinguishing soils are not necessarily the same for different classification systems. Soil texture is a good example of the problems involved in correlating classifications between two or more systems. Texture describes the proportion of different size classes of the mineral part of the soil. For the same soil, texture-class names can differ depending on the classification system used. Even if the names are the same, the limits often differ.

The problem continues with particle-size classes. For example, clay is defined as <0.002 mm in diameter by some systems and <0.005 mm by others. Other physical, chemical, and biological characteristics have similar discrepancies between systems which makes one to one correlation between systems nearly impossible unless a detailed soil description is available.

The Finnish classification system is particular for the reason it depends on numerous parameter. We have to know in order to classify a Finnish soil: The organic content, the liquid limit, percentage of the different grain's size contained and the geological history of the site where the sample comes from.

The tests used in the laboratory to get these characteristics are:

- Organic content (800°C heating)
- Liquid limit: fall cone test, Casagrande test. (see appendix 2 below)
- Percentage of the different grain's size: densimeter test.

Even if the methods and the limits differ from a classification to another the characteristics considered to determine the class of the soil are the same e.g. the unified soil classification.

First and/or second letters	Definition	Second letter	Definition
G	gravel	**P**	Poorly graded (well sorted)
S	Sand	**W**	well graded (poorly sorted)
M	Silt	**H**	High plasticity
C	clay	**L**	Low plasticity
O	Organic		

Table 1'' The unified soil classification

Major divisions			Group symbols	Group name
Coarse grained soils more than 50% retained on No.200 sieve	Gravel > 50% of coarse fraction retained on No.4 sieve	clean gravel	**GW**	well graded gravel, fine to coarse gravel
			GP	poorly graded gravel
		gravel with fines	**GM**	salty gravel
			GC	clayey gravel
	Sand ≥ 50% of coarse fraction passes No.4 sieve	clean sand	**SW**	well graded sand, fine to coarse sand
			SP	poorly-graded sand
		sand with fines	**SM**	silty sand
			SC	clayey sand
Fine grained soils more than 50% passes No.200 sieve	silt and clay liquid limit < 50	Inorganic	**ML**	Silt
			CL	Clay
		Organic	**OL**	organic silt, organic clay
	silt and clay liquid limit ≥ 50	Inorganic	**MH**	silt of high plasticity, elastic silt
			CH	clay of high plasticity, fat clay
		Organic	**OH**	organic clay, organic silt
Highly organic soils			**PT**	Peat

Other tests

Fall cone test

Operating method

A slice of the sample is cut and put under a loaded cone. The gauge is set to zero and the cone is brought just upon the surface of the sample. The principle is then to let the loaded cone fallen and to check the value of the cone driving in, on the gauge.

NB: the load applied depends on the estimated undrained shear strength forces of the sample.

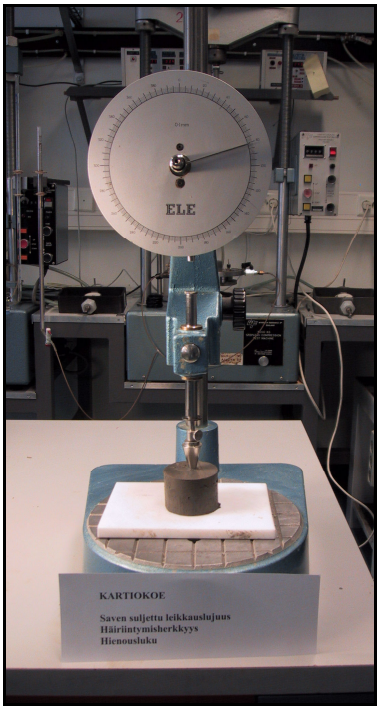

Figure 4'' Fall cone test apparatus

Results processing

The penetration value can be now converted into a value for undrained shear strength force thanks to tables. We get thus a value of undrained shear strength force as an estimation confirmed later by the unconfined compression stress. The results are often higher for this test than for the unconfined compression test but it's a good means to certify the results.

The penetration value can also be converted to assess the liquid limit of the sample, indeed the Casagrande apparatus is nowadays only used to verify the value obtained. The reason of this is the disparate results got with this test.

We can note that the sensitivity of a sample can also be estimated with this test. To assess this characteristic we proceed the same way but on a remoulded sample and we compare the value with the one obtained with an undisturbed sample.

Unconfined compression test

Operating method

The goal of this test is also to get the undrained shear strength value. A sample from the piston sampler is put under a load. The borders of the sample are let free to move. The load is set by applying a constant strain rate on the sample until the failure. During this test the load applied and the settlements of the samples are checked.

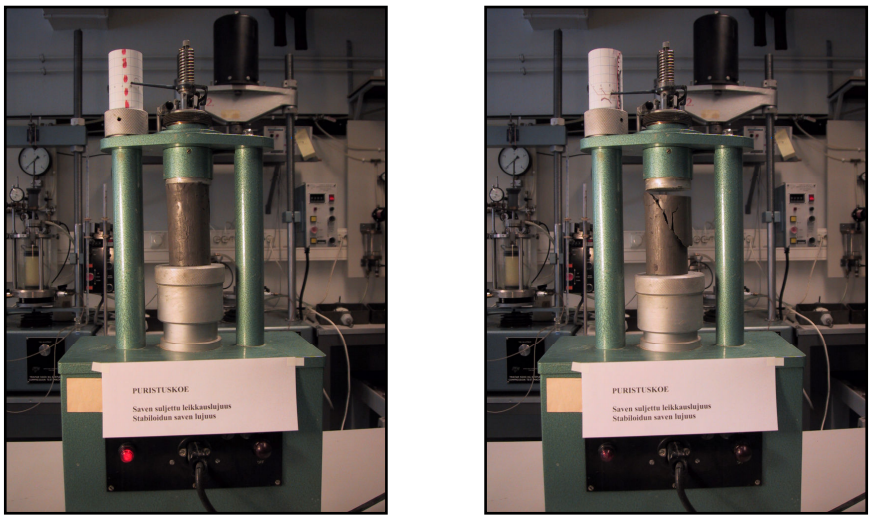

Figure 5" Unconfined compression test

Results processing

To process the data we plot the load-displacement curve. Thus we can determinate the undrained shear strength of the soil and compare it to the one obtained with the Fall cone test.

APPENDIX 3

Taasia 21D1

Parameters:

- Dimensions of the sample:
  - H_{init} =20 mm
  - A = 2000 mm^2

- $\sigma_1 = \sigma$ applied = 200 kPa
- $\sigma_{10} = \sigma$ applied at the previous load step = 100 kPa
- h_0 = height of the sample at the end of the previous load step = 19,172 mm

- λ^* = 0,256
- κ^* = 7,81.E-3 ($\lambda/\kappa = 32,7$)
- μ^* =5,348.E-3
- k = 5.E-6 m/day
- e_0 = 2,7
- $POP = \left|\sigma_p - \sigma_{yy}^{'0}\right| = \left|90 - 0\right| = 90kPa$

- c = 2 kPa
- φ = 24˚
- ψ = 0˚

- γ_{sat} = 14,6 kN/m^3
- γ_{unsat} = 7,3 kN/m^3

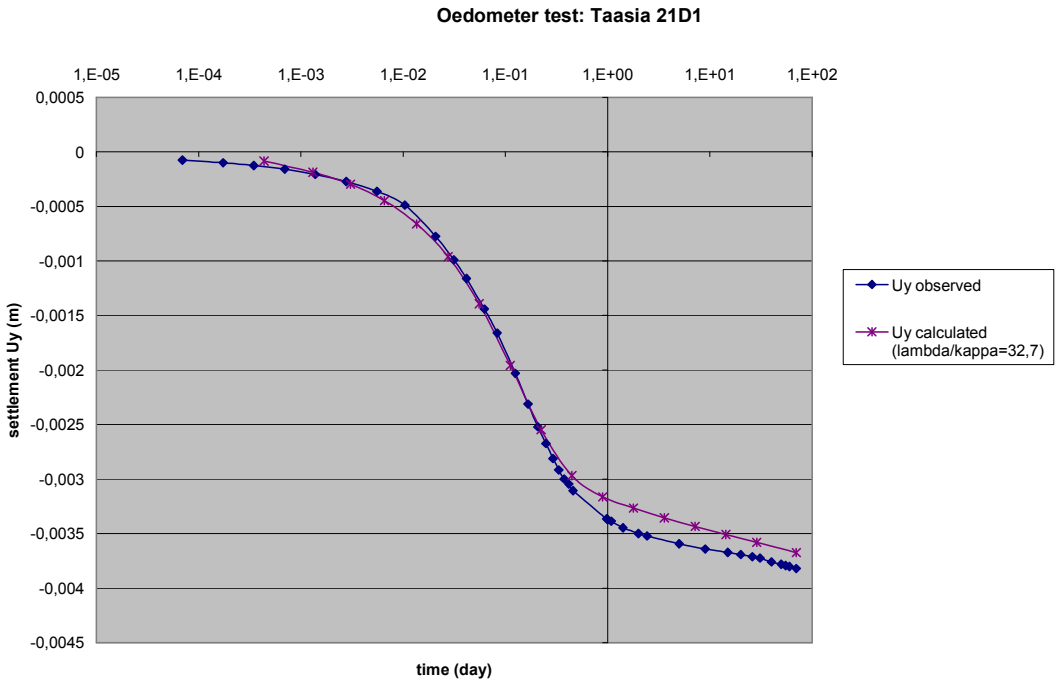

Figure 1''' Computed/observed settlement of the 21 oedometer test's sample

Error at 70 days [%]: 3,9

Taasia 26B1

Parameters:

- Dimensions of the sample:
  - H_{init} =20 mm
  - A = 2000 mm^2

- $\sigma_1 = \sigma$ applied = 200 kPa
- $\sigma_{10} = \sigma$ applied at the previous load step = 100 kPa
- h_0 = height of the sample at the end of the previous load step = 18,757 mm

- λ^* = 2,031.E-1
- κ^* = 2,381.E-2
- μ^* =5,25.E-3
- k = 4.E-6 m/day

- e_0 = 2,52
- $POP = \left|\sigma_p - \sigma_{yy}^{'0}\right| = \left|100 - 0\right| = 100kPa$

- c = 2 kPa
- φ = 24˚
- ψ = 0˚

- γ_{sat} = 14,77 kN/m^3
- γ_{unsat} = 7,64 kN/m^3

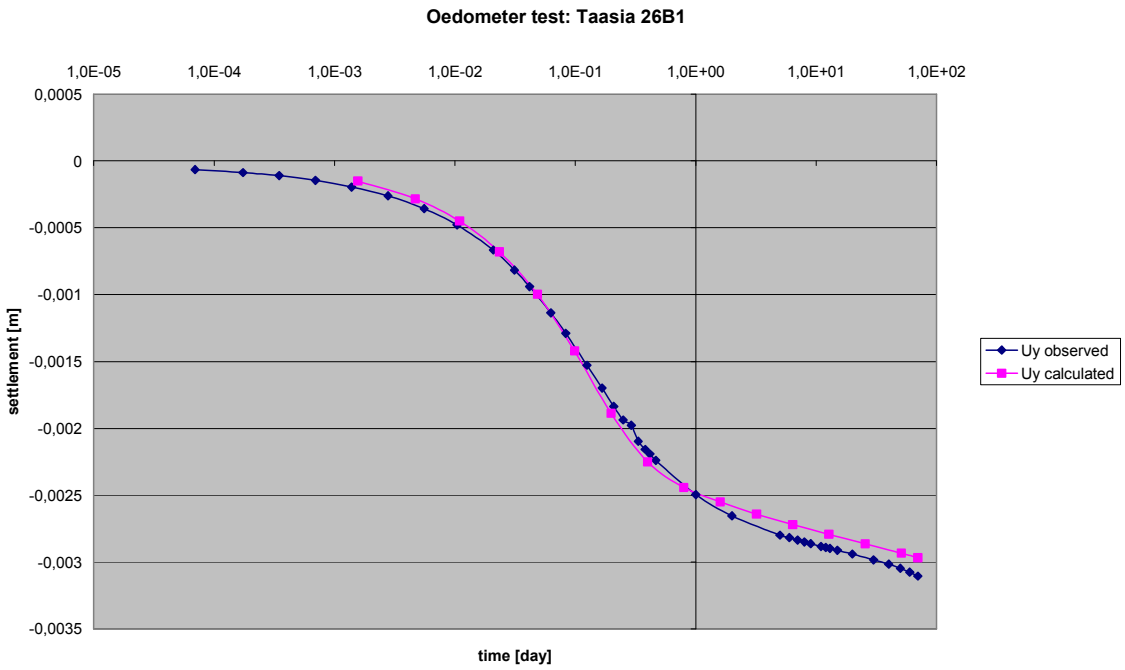

Figure 2''' Computed/observed settlement of the 26 oedometer test's sample

Error at 70 days [%]: 4,3

Vanttila 4452

Parameters:

- Dimensions of the sample:
  - H_{init} =15 mm
  - A = 1380 mm^2

- $\sigma_1 = \sigma$ applied = 42,4 kPa
- $\sigma_{10} = \sigma$ applied at the previous load step = 21,4 kPa
- h_0 = height of the sample at the end of the previous load step = 13,606 mm

- λ^* = 2,214.E-1
- κ^* = 5,714.E-3
- μ^* =7,687.E-3
- k = 3,119.E-5 m/day
- e_0 = 3,17
- $POP = \left|\sigma_p - \sigma_{yy}^{'0}\right| = \left|13 - 0\right| = 13kPa$

- c = 2 kPa
- φ = 24˚
- ψ = 0˚

- γ_{sat} = 13,56 kN/m^3
- γ_{unsat} = 6,36 kN/m^3

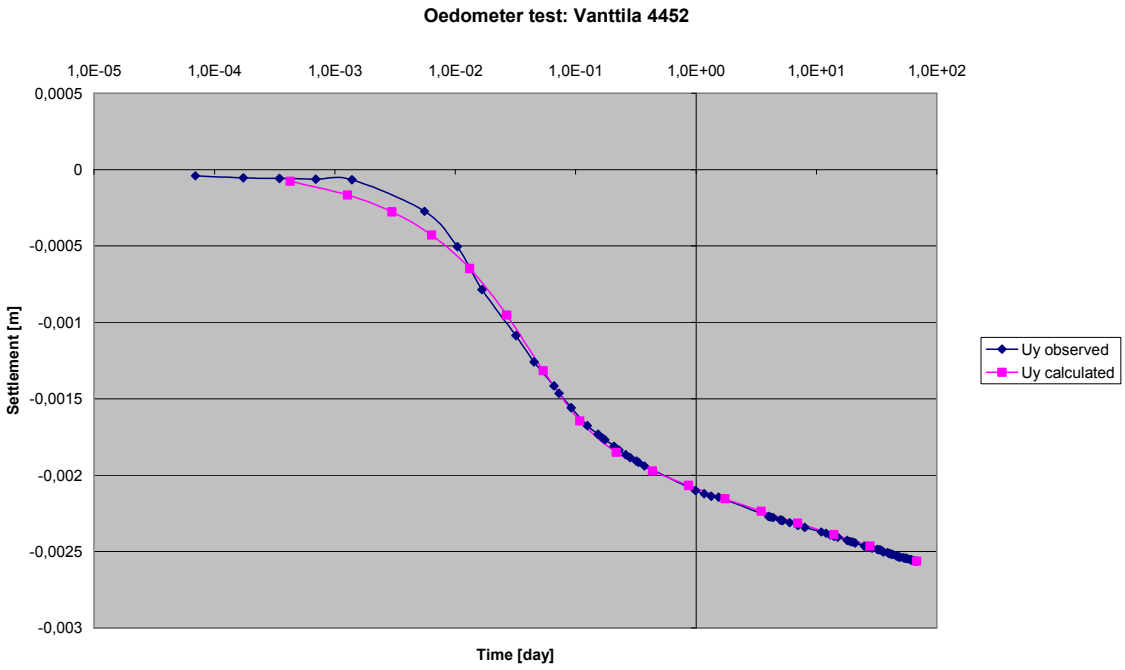

Figure 3''' Computed/observed settlement of the 4452 oedometer test's sample

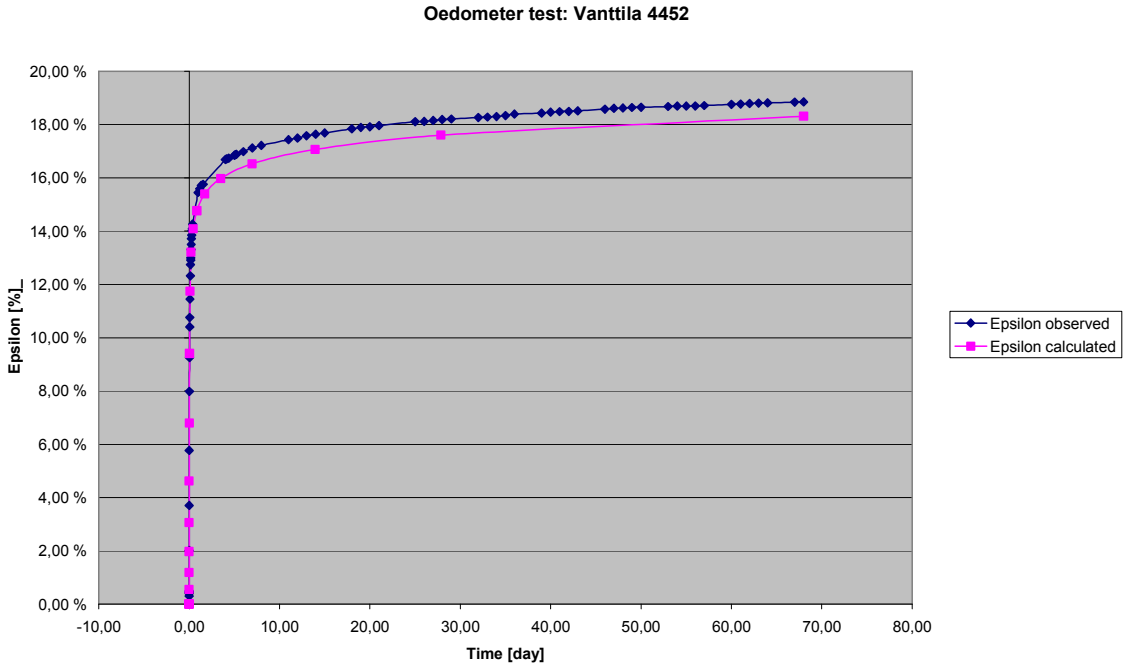

Figure 4''' Computed/observed strain of the 4452 oedometer test's sample

Error at 68 days [%]: 2,9

Vanttila 4453

Parameters:

- Dimensions of the sample:
  - H_{init} =15 mm
  - A = 1380 mm^2

- $\sigma_1 = \sigma$ applied = 42,8 kPa
- $\sigma_{10} = \sigma$ applied at the previous load step = 21,4 kPa
- h_0 = height of the sample at the end of the previous load step = 14,352 mm

- λ^* = 1,683.E-1
- κ^* = 1,359.E-2
- μ^* =1,077.E-2
- k = 1,607.E-5 m/day
- e_0 = 3,037
- $POP = \left|\sigma_p - \sigma_{yy}^{'0}\right| = \left|25 - 0\right| = 25kPa$

- c = 2 kPa
- φ = 24˚
- ψ = 0˚

- γ_{sat} = 14,12 kN/m^3
- γ_{unsat} = 6,62 kN/m^3

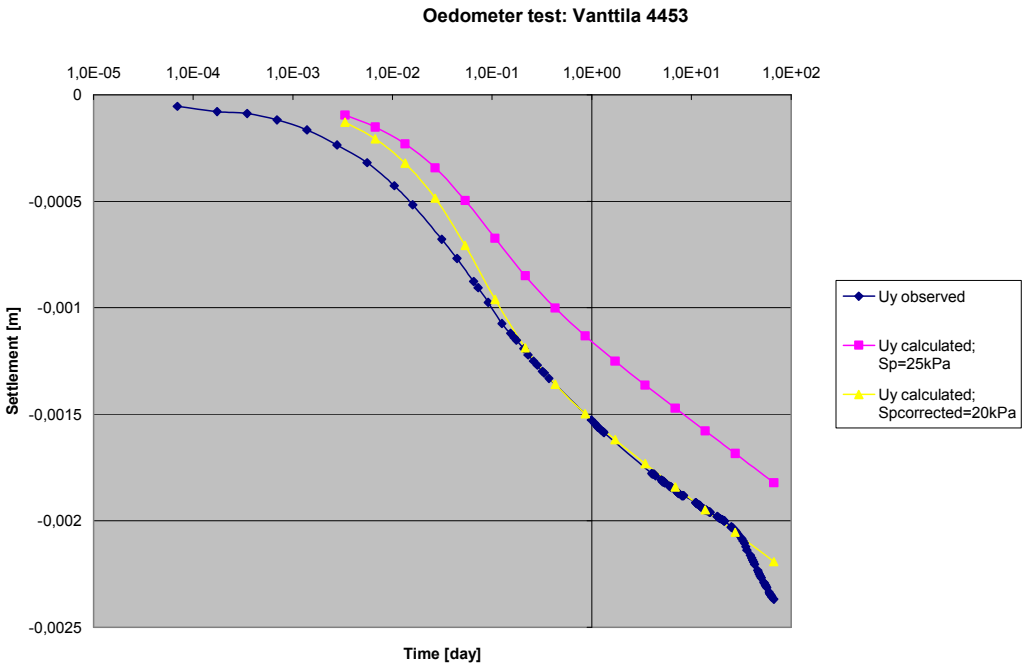

Figure 5''' Computed/observed settlement of the 4453 oedometer test's sample

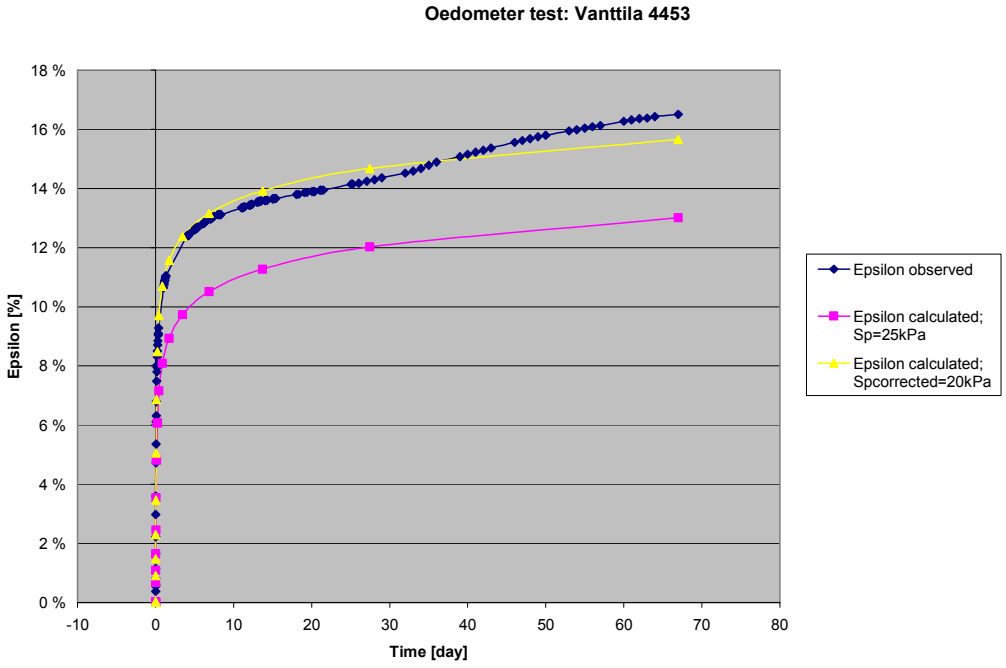

Figure 6''' Computed/observed strain of the 4453 oedometer test's sample

Table 1''' Vanttila 4453, Final error

Preconsolidation pressure - σp	Error [%]
25	21,2
20	5,1

Perno 116

Parameters:

- Dimensions of the sample:
  - H_{init} =19 mm
  - A = 4570 mm^2

- $\sigma_1 = \sigma$ applied = 12,5 kPa
- $\sigma_{10} = \sigma$ applied at the previous load step = 6,25 kPa
- h_0 = height of the sample at the end of the previous load step = 17,60 mm

- λ^* = 1,218.E-1
- κ^* = 1,812.E-2
- μ^* =1,0857.E-2
- k =7,4649.E-5 m/day
- e_0 = 5,6
- $POP = \left|\sigma_p - \sigma_{yy}^{'0}\right| = \left|6 - 0\right| = 6kPa$

- c = 2 kPa
- φ = 24˚
- ψ = 0˚

- γ_{sat} = 12,58 kN/m^3
- γ_{unsat} = 4,09 kN/m^3

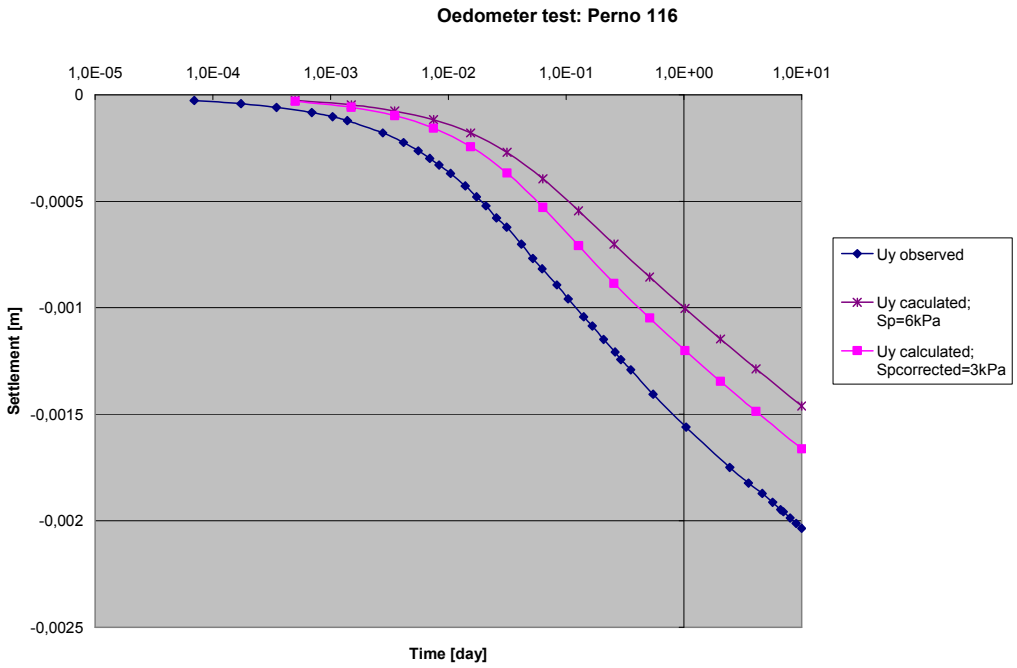

Figure 7''' Computed/observed settlement of the 116 oedometer test's sample

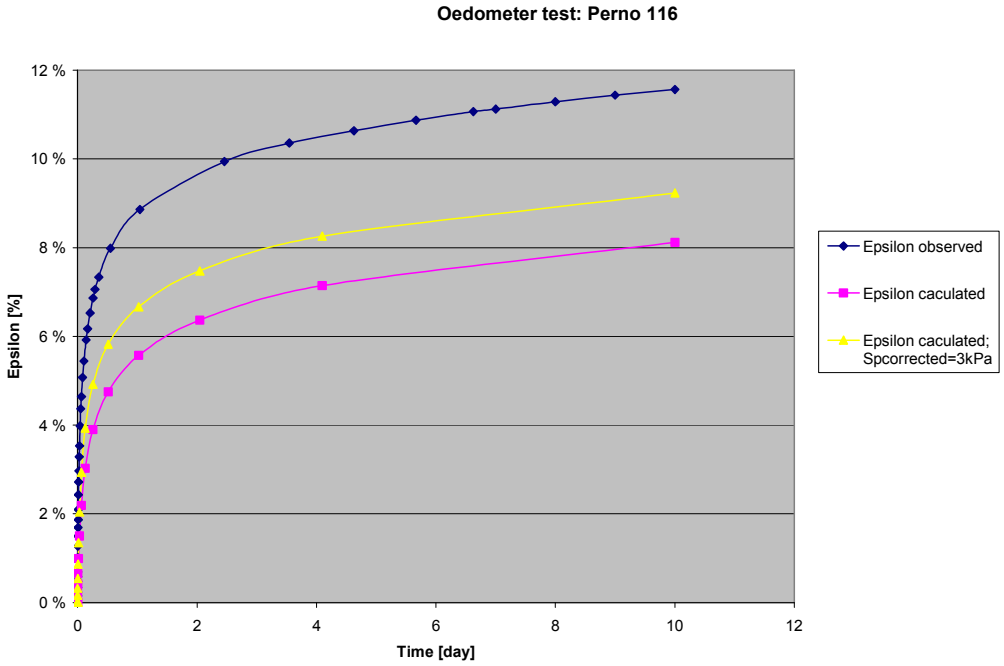

Figure 8''' Computed/observed strain of the 116 oedometer test's sample

Table 2''' Perno 116, sigma1 = 12,5kPa, Final error

Preconsolidation pressure - σp	Error at 10 days [%]
3	20
6	29

Suurpelto 4532

Parameters:

- Dimensions of the sample:
  - H_{init} =15 mm
  - A = 1590 mm^2

- $\sigma_1 = \sigma$ applied = 25 kPa
- $\sigma_{10} = \sigma$ applied at the previous load step = 12,5 kPa
- h_0 = height of the sample at the end of the previous load step = 14,11 mm

- λ^* = 1,4858.E-1
- κ^* = 7,1668.E-3
- μ^* =1,239.E-2
- k = 1,4688.E-5 m/day
- e_0 = 4,665
- $POP = \left|\sigma_p - \sigma_{yy}^{'0}\right| = \left|9 - 0\right| = 9kPa$

- c = 2 kPa
- φ = 24˚
- ψ = 0˚

- γ_{sat} = 12,84 kN/m^3
- γ_{unsat} = 4,45 kN/m^3

For this test the value of C_α used is the one obtained directly from experimentation as modelling the behavior during secondary compression (varying with the stress) has not been possible. $C_\alpha = 2{,}85\%$.

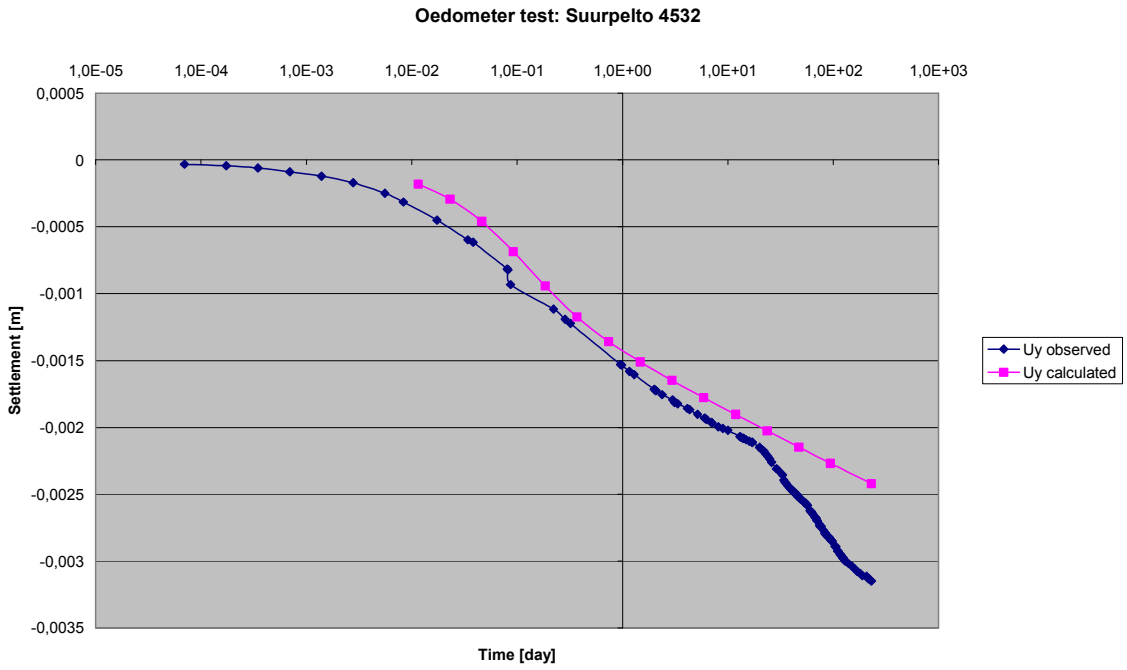

Figure 11''' Computed/observed settlement of the 4532 oedometer test's sample

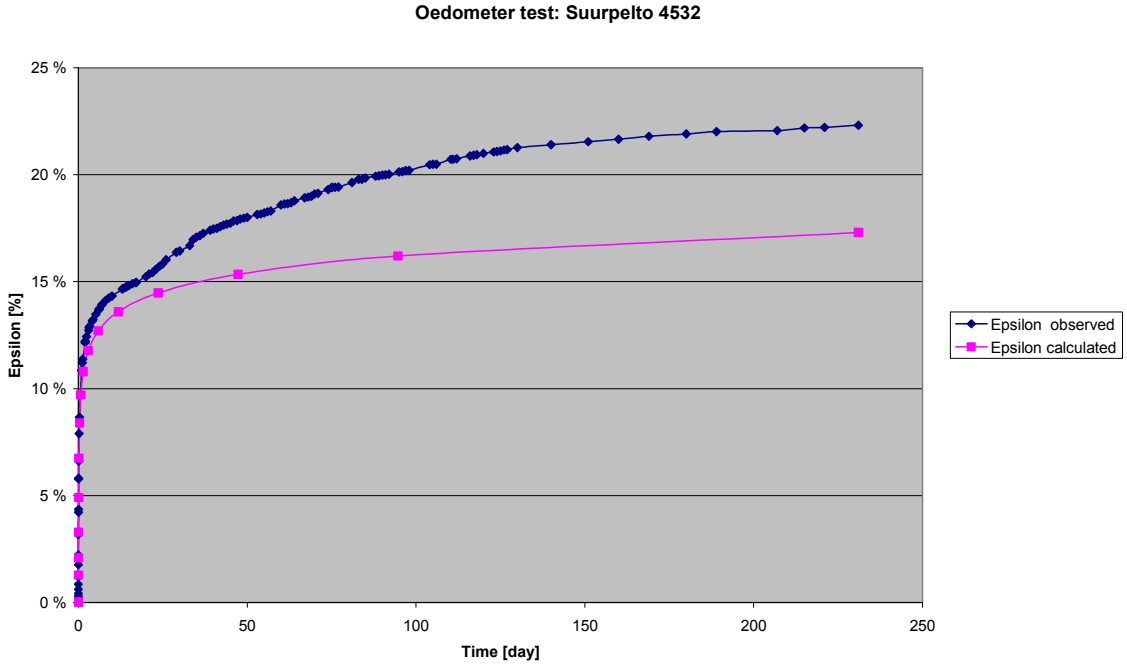

Figure 12''' Computed/observed strain of the 4532 oedometer test's sample

Error at 231 days [%]: 22,4

Suurpelto 4533

Parameters:

- Dimensions of the sample:
  - H_{init} =15 mm
  - A = 1590 mm^2

- $\sigma_1 = \sigma$ applied = 25 kPa
- $\sigma_{10} = \sigma$ applied at the previous load step = 12,5 kPa
- h_0 = height of the sample at the end of the previous load step = 14,588 mm

- λ^* = 1,339.E-1
- κ^* = 1,879.E-2
- μ^* = 5,739.E-3
- k = 9,063.E-6 m/day
- e_0 = 2,846
- $POP = \left|\sigma_p - \sigma_{yy}^{'0}\right| = \left|20 - 0\right| = 20kPa$

- c = 2 kPa
- φ = 24˚
- ψ = 0˚

- γ_{sat} = 13,89 kN/m^3
- γ_{unsat} = 6,43 kN/m^3

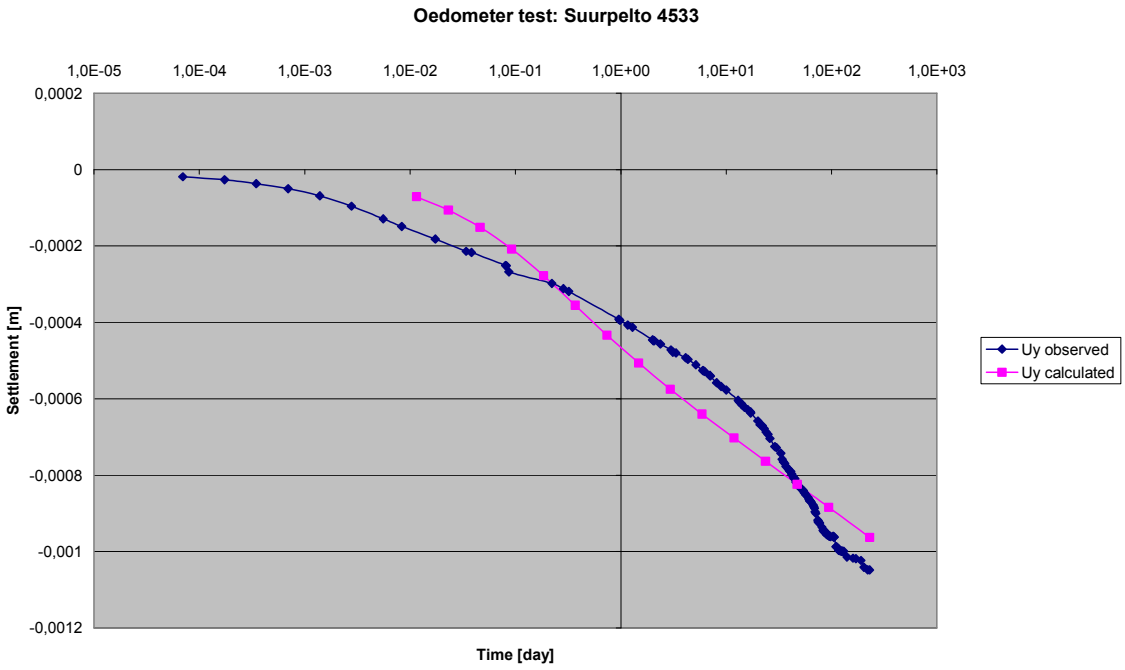

Figure 13''' Computed/observed settlement of the 4533 oedometer test's sample

One can notice a huge difference between the model and what is actually observed this is due to the strange behavior of this clay and how we have modelled it. Indeed the primary consolidation occurs very late so the first modelling line of the Casagrande's construction is very steep. (c.f plot below Casagrande's construction)

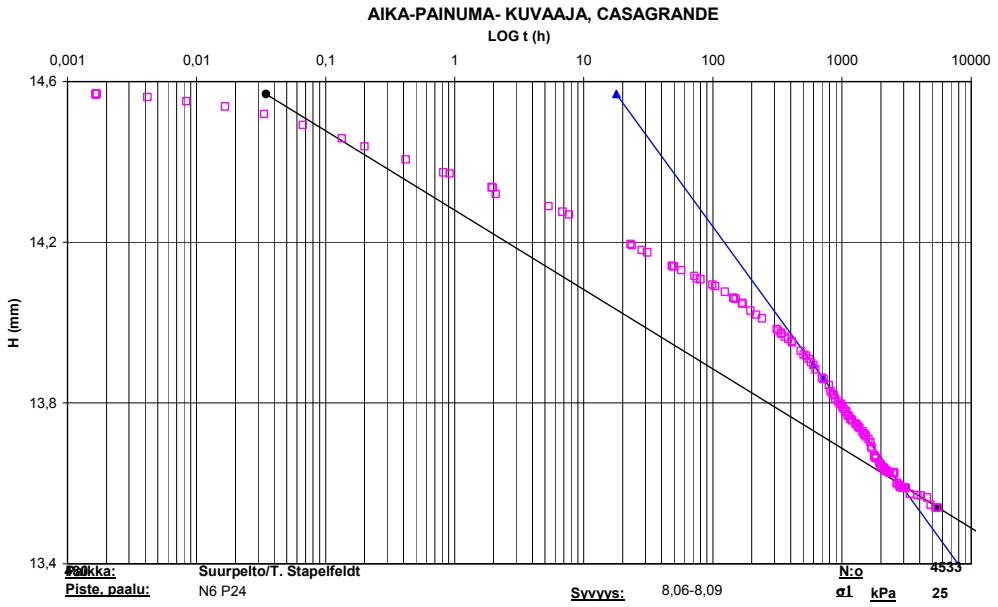

Figure 14''' Particular settlement-log(t) curve observed for 4533 oedometer test

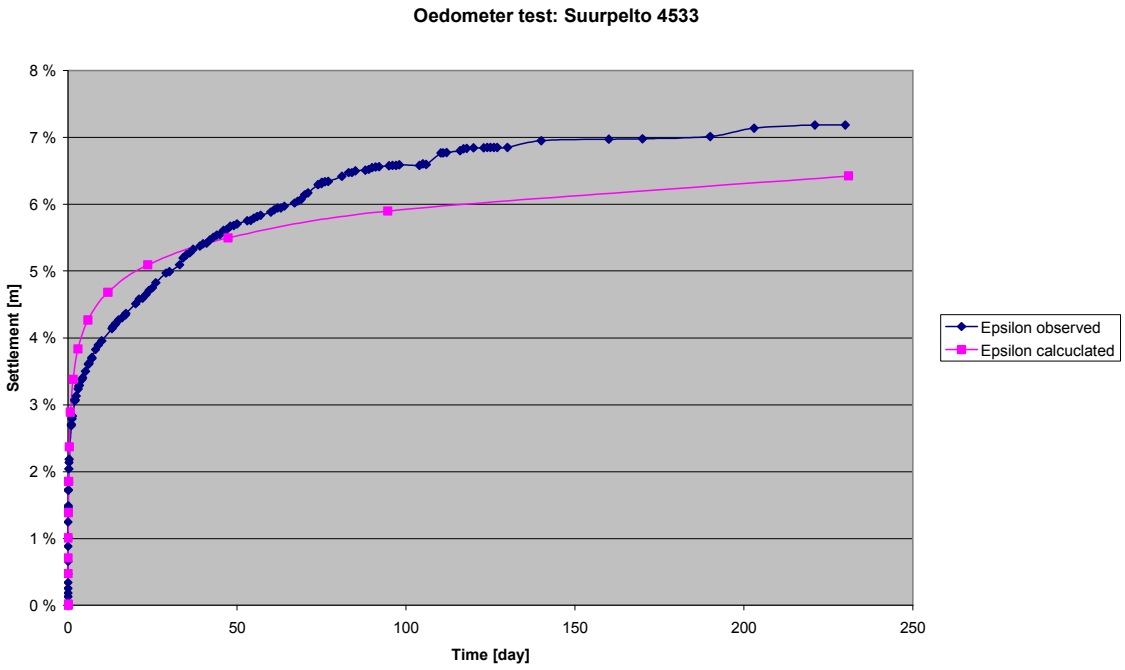

Figure 15”’ Computed/observed strain of the 4533 oedometer test’s sample